Turbulence in the atmosphere: nonstationary, anisotropic and inhomogeneous.

What can we do?

Howto in atmospheric models?

Szymon Malinowski
together with collaborators and students

University of Warsaw

2025-02-10

UNIWERSYTET WARSZAWSKI

UNIVERSITY OF WARSAW | INSTITUTE OF GEOPHYSICS

Institute of Geophysics Studies Research Employees

Multilevel Optical Storage, Dynamic Light Modulation, and Polarization Control in Filamented Memristor System

Korneluk A., Stefaniuk T.

• • •

RESEARCH GROUPS

STUDIES

METEO STATION

POPULARIZATION

INFORMATION SERVICE

Current Archive

Feb. 7, 2025
Dissipation Scaling with a Variable Cε Coefficient in the Stable Atmospheric Boundary Layer
Wacławczyk M., Nzotungishaka J., Jędrejko P., Sarkar J., and Malinowski S.P.

Feb. 4, 2025
Efficient Photoelectrochemical Reduction of CO2 in Seawater with Cheap and Abundant Cu2O/Al2O3/TiO2 Electrode
Parzuch A., Kuder K., Nikiforow K., Wróbel P., Kaproń G., Bieńkowski K., Solarska R.

Jan. 24, 2025
Multilevel Optical Storage, Dynamic Light Modulation, and Polarization Control in Filamented Memristor System
Korneluk A., Stefaniuk T.

EVENTS

Current Archive

Feb. 20, 2025, 10 a.m., ul. Pasteura 5, 0.22C
Defense of doctoral thesis
mgr inż. Stanisław Król
Instytut Geofizyki, Wydział Fizyki, Uniwersytet Warszawski

Feb. 26, 2025, 1:15 p.m., ul. Pasteura 5, sala 2.07
Vision science - seminar
Dr n. med. Paweł Rogala
Klinika Nowotworów Tkanek Miękkich Kości i Czerniaków

March 26, 2025, 1:15 p.m., on-line
Vision science - seminar
dr inż. Paweł Hottowy
Akademia Górniczo-Hutnicza

Turbulence:

- no good definition;

- for atmospheric modelers: something subgrid;

- for pilots and passengers: variations of the flow affecting flight of an aircraft;

- in fluid dynamics: fluid motion characterized by chaotic changes in pressure and flow velocity;

- in this talk: atmospheric turbulence is the air motion of scales of hundreds of meters and below important for transport processes and mixing.

We will focus on substantial velocity and temperature fluctuations present in the atmospheric boundary layer and higher, in the free atmosphere, especially within and around clouds.

Atmosphere:

- gas layer around a planet, here around the Earth;

Weather:

- state of the atmosphere in a given moment above a certain location in the Earth;

Climate:

- characteristic properties of the climatic system (atmosphere, ocean, Earth’s surface) resulting from external forcings and internal responses (feedbacks) within the climate system, in simplified approach statistics of weathers at given forcings.

Weather and climate models: mathematical and computational models of weather and climate based on fundamental laws of physics with necessary simplifications and parametrizations of unresolved processes.

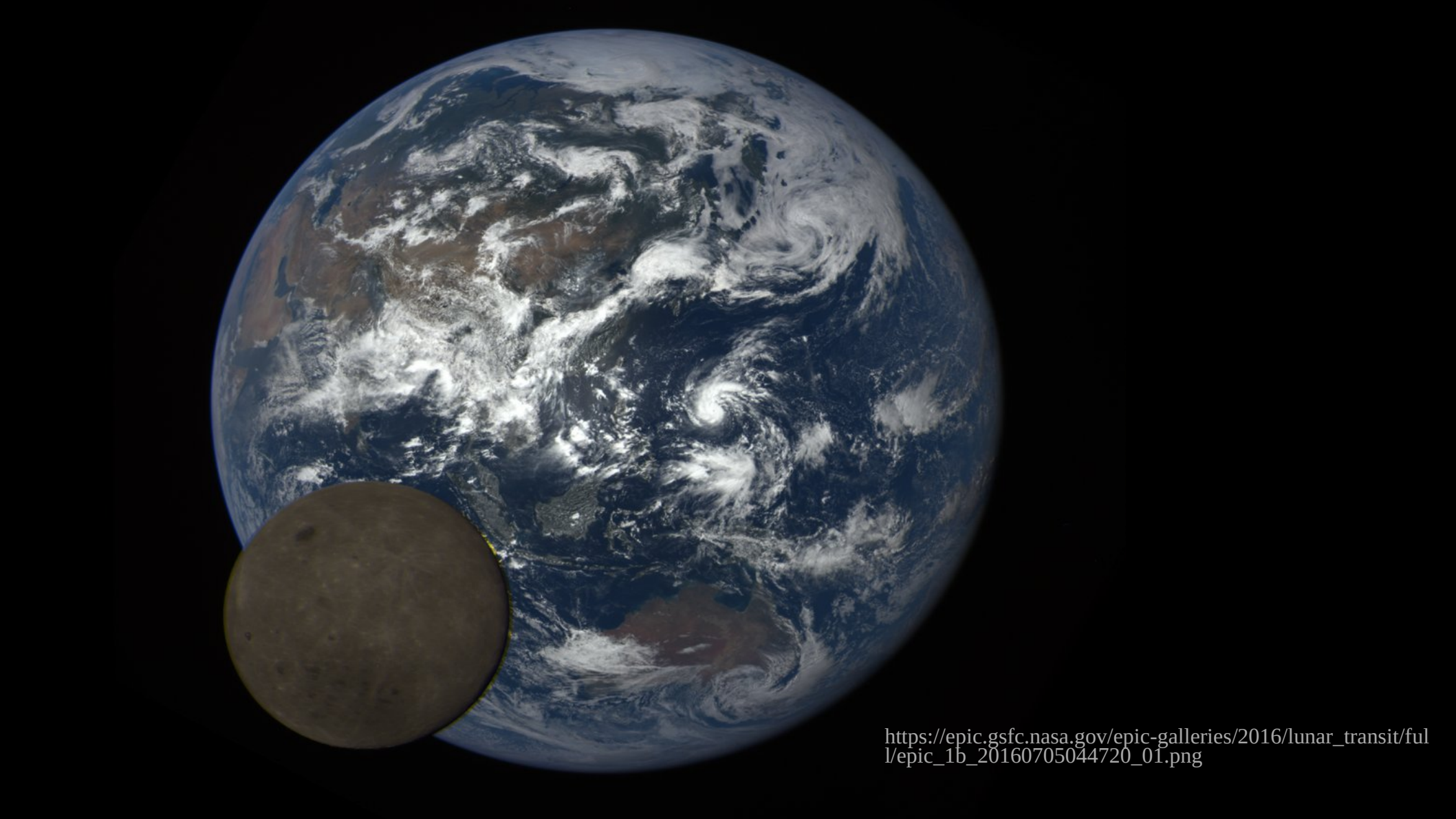

https://epic.gsfc.nasa.gov/epic-galleries/2016/lunar_transit/full/epic_1b_20160705044720_01.png

Earth's temperature depends on energy balance: absorption of Solar energy ΔQ_S and emission of energy to space ΔQ_C

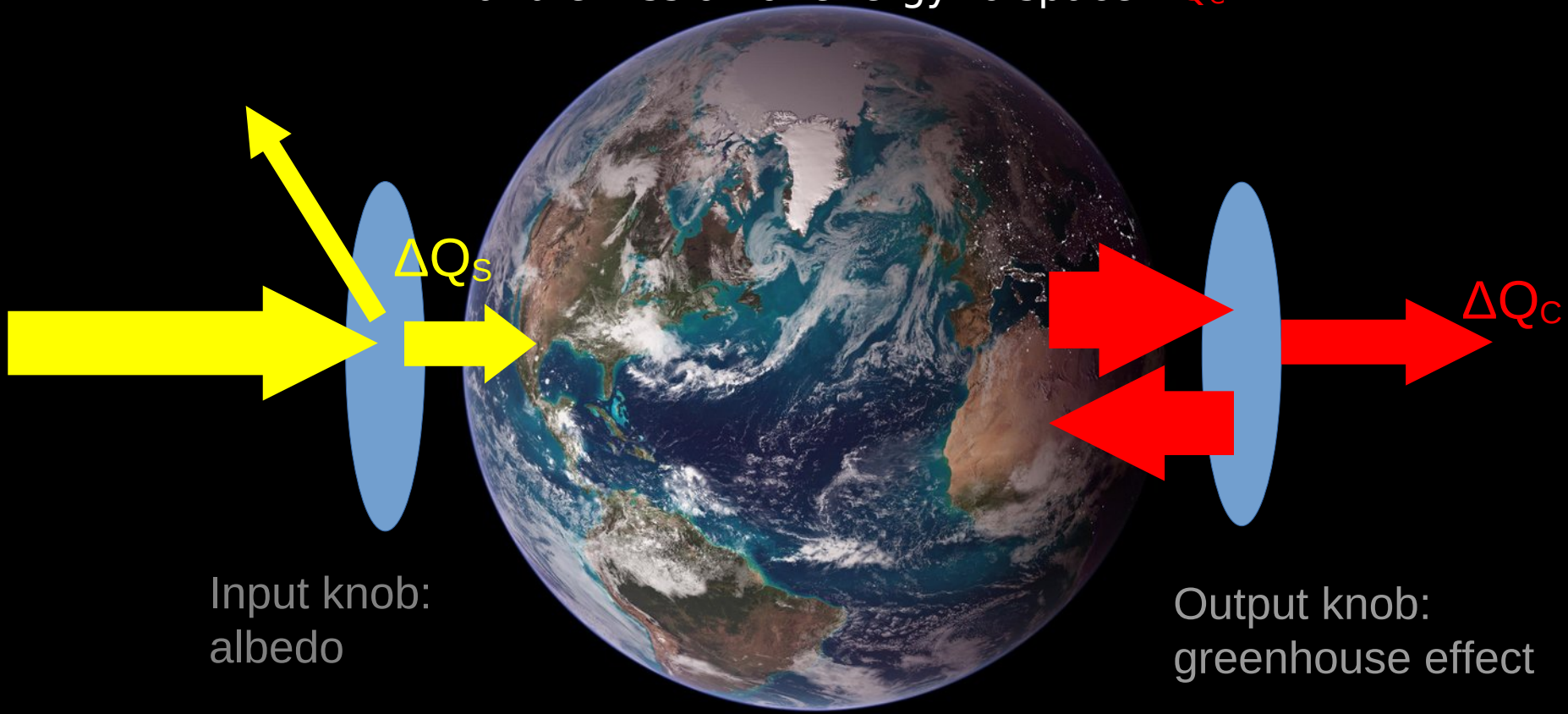

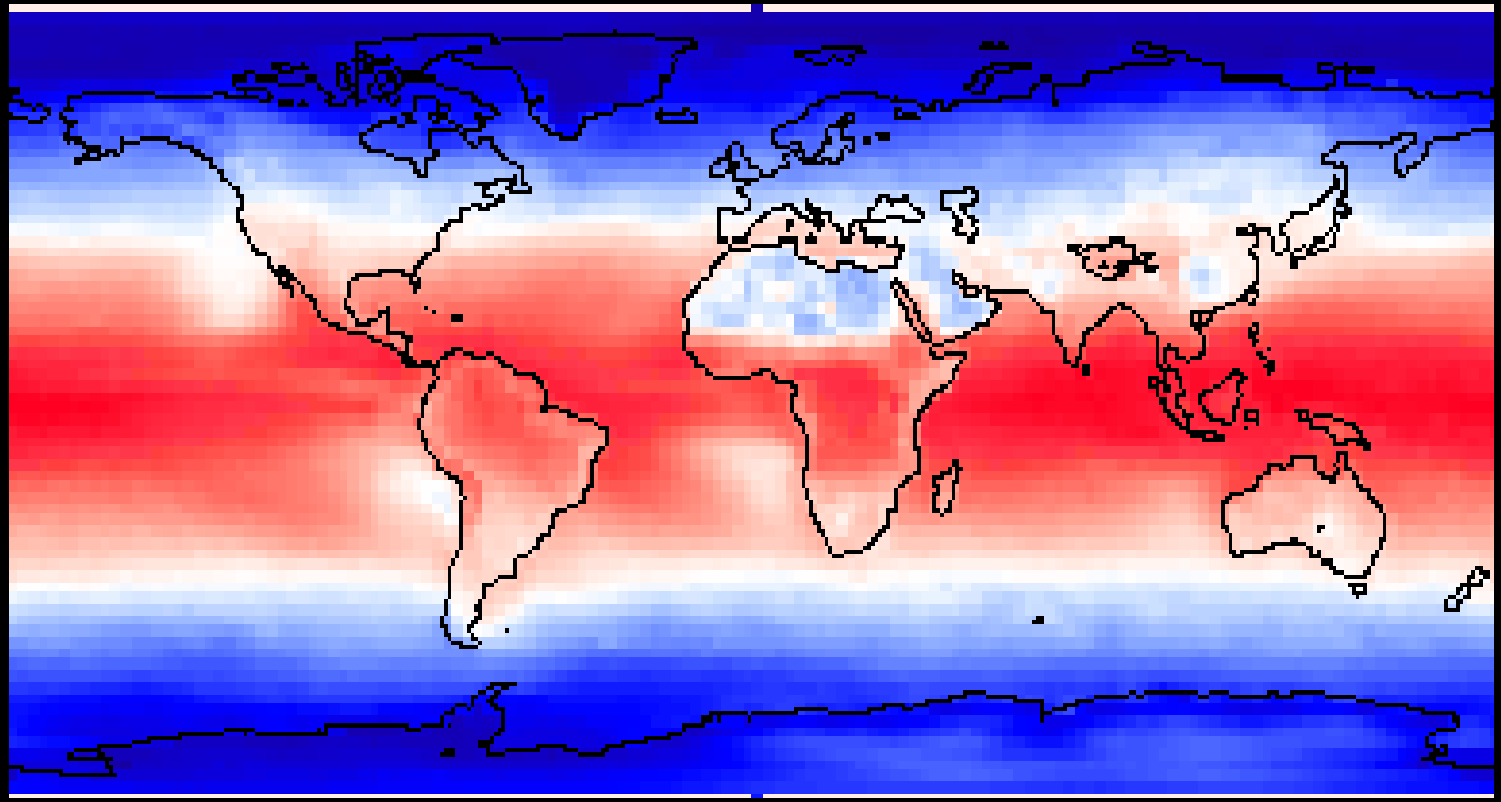

Radiative balance
-long term average

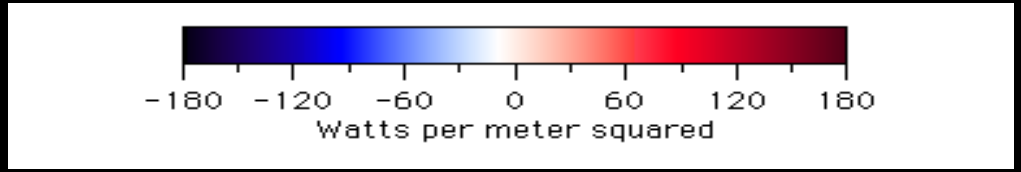

earthobservatory.nasa.gov

Short- and longwave radiation

Average minute values of the shortwave and longwave radiation in W/m2, reaching the earth's surface. Shortwave and longwave radiation is measured by the CM22 pyranometer and the CNR4 pyrgeometer, respectively. Both instruments are installed on the LTR platform. Shortwave radiation, i.e. solar radiation, contains diffuse component (solid green line) and total component (solid blue line). Dashed blue and green lines mean total and diffuse radiation obtained using a radiation transfer model for a cloudless sky.

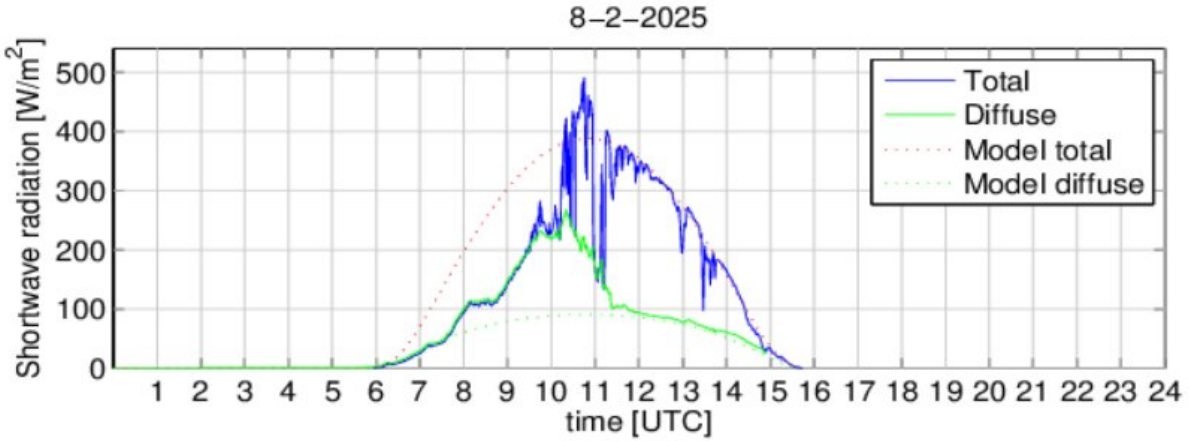

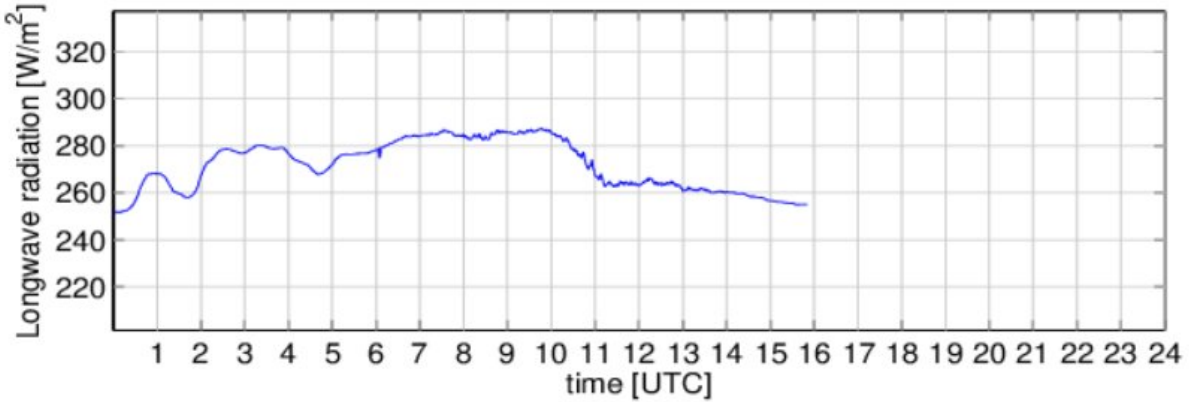

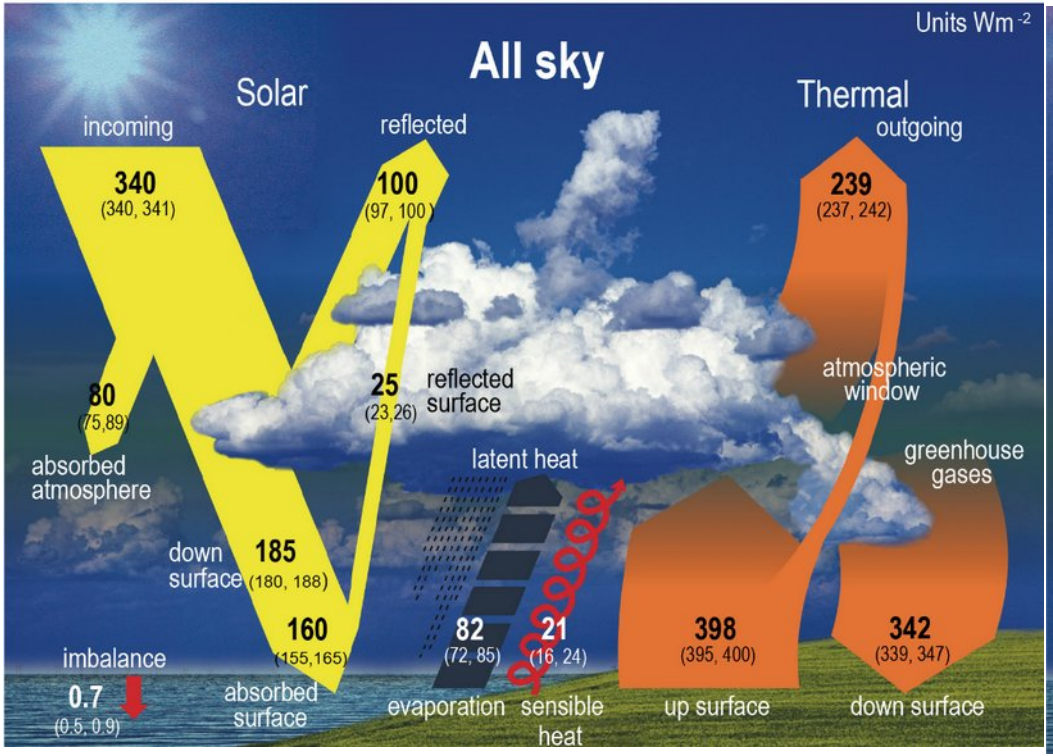

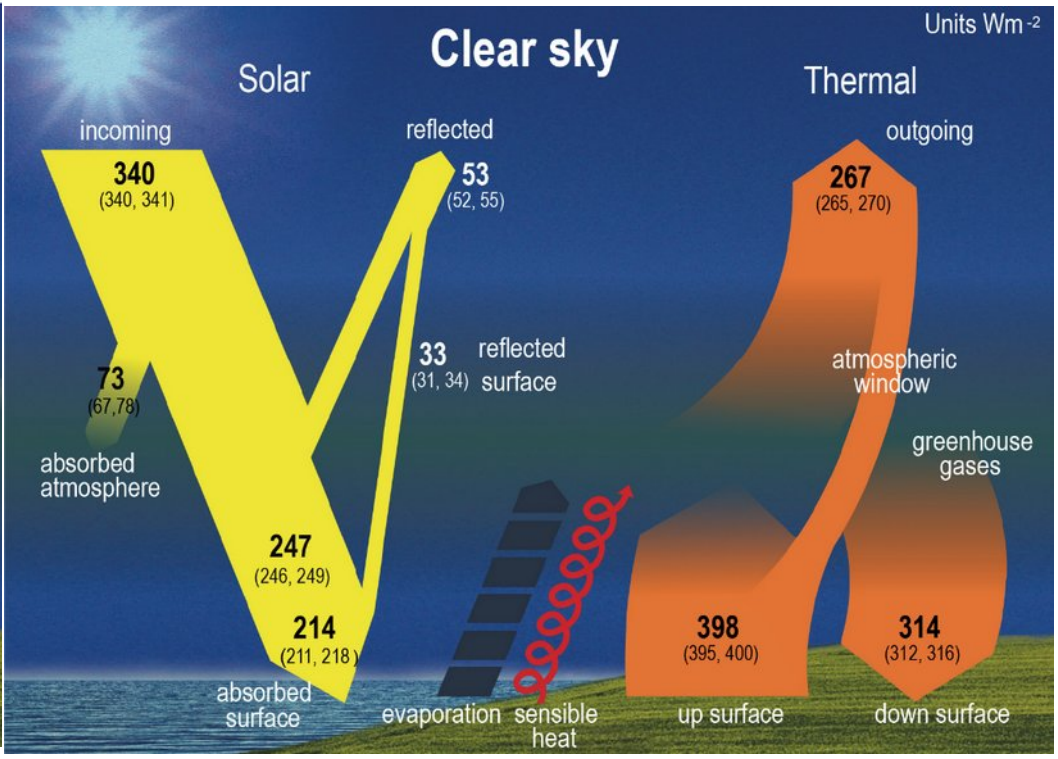

Representation of the global mean energy budget of the Earth (left panel), and its equivalent without considerations of cloud effects (lright panel). Numbers indicate best estimates for the magnitudes of the globally averaged energy balance components in W m–2 together with their uncertainty ranges in parentheses, representing climate conditions at the beginning of the 21st century. The cloud-free energy budget is not the one that Earth would achieve in equilibrium when no clouds could form. It rather represents the global mean fluxes as determined solely by removing the clouds .

Climate/weather modeling: construction of a virtual planet based on laws of physics.

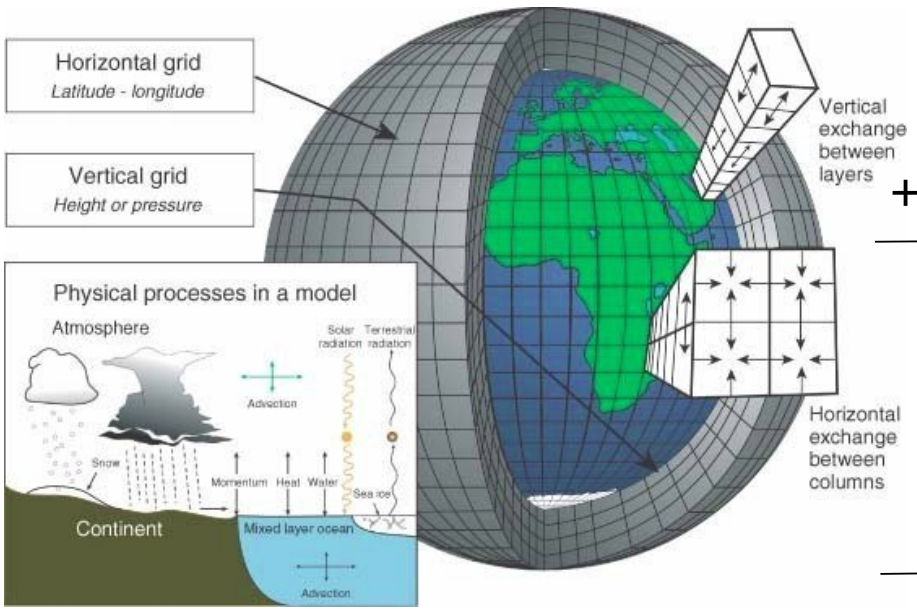

hydrodynamcs
thermodynamics
radiative transfer
constitutive equations
atmosphere-ocean-biosphere exchange
surface processes and interactions
\+ chemistry

---

model equations

* numeric code
* feeding with data
* computing facility

---

virtual planet ready for experimenting

Edwards Paul N.. History of climate modeling.
WIREs Clim Change
2011, 2: 128-139. doi: 10.1002/wcc.95

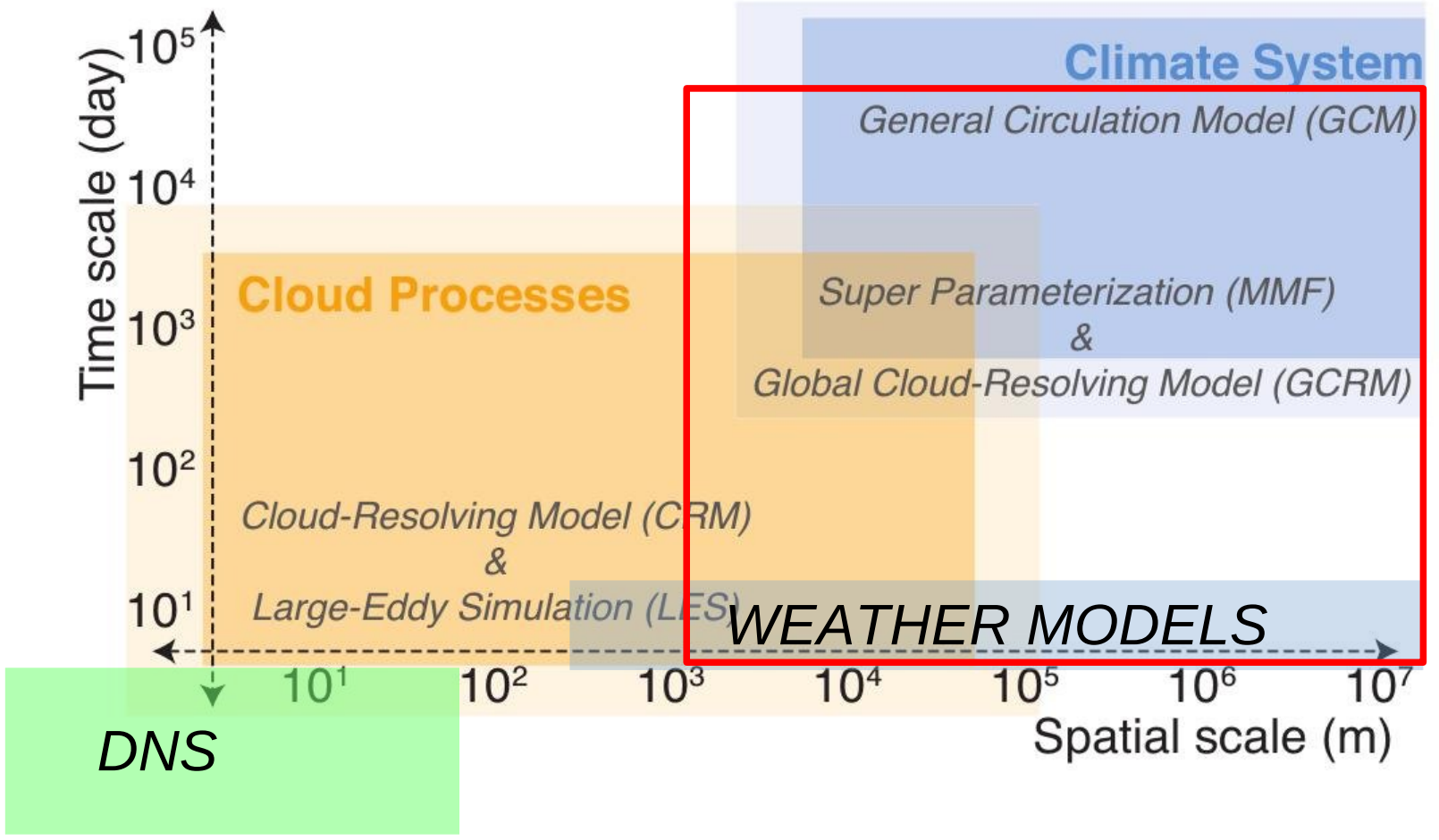

small-scale flow models ⟷ climate and weather models

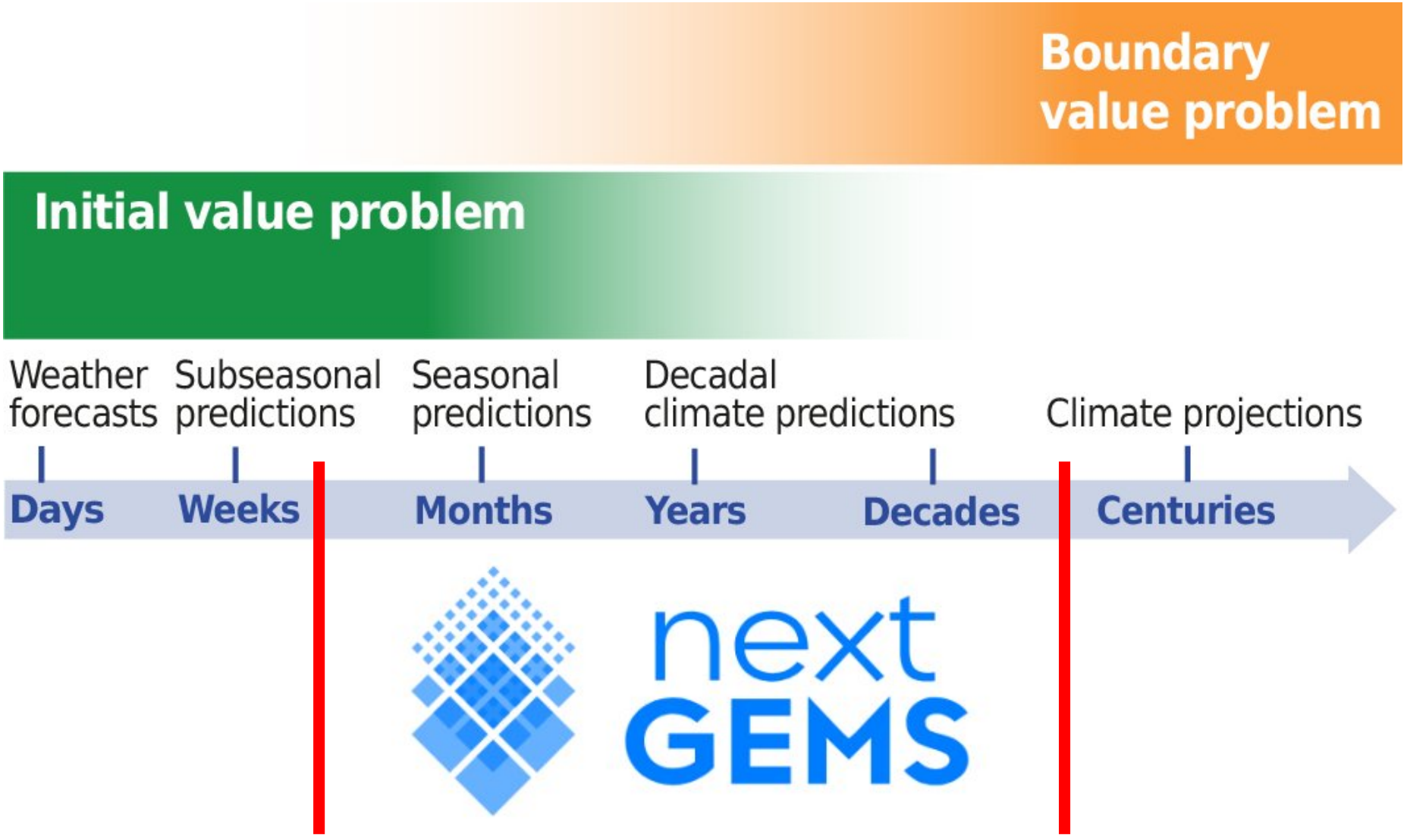
Boundary value problem
Initial value problem
Weather forecasts
Subseasonal predictions
Seasonal predictions
Decadal climate predictions
Climate projections
Days
Weeks
Months
Years
Decades
Centuries
next GEMS

Which problems are crucial for weather and climate modeling?
- scale range
- a variety of processes, from fluid dynamics, thermodynamics, radiative transfer, microphysics, ainsotropy…
Let’s have a look into details and find some key processes related to turbulence

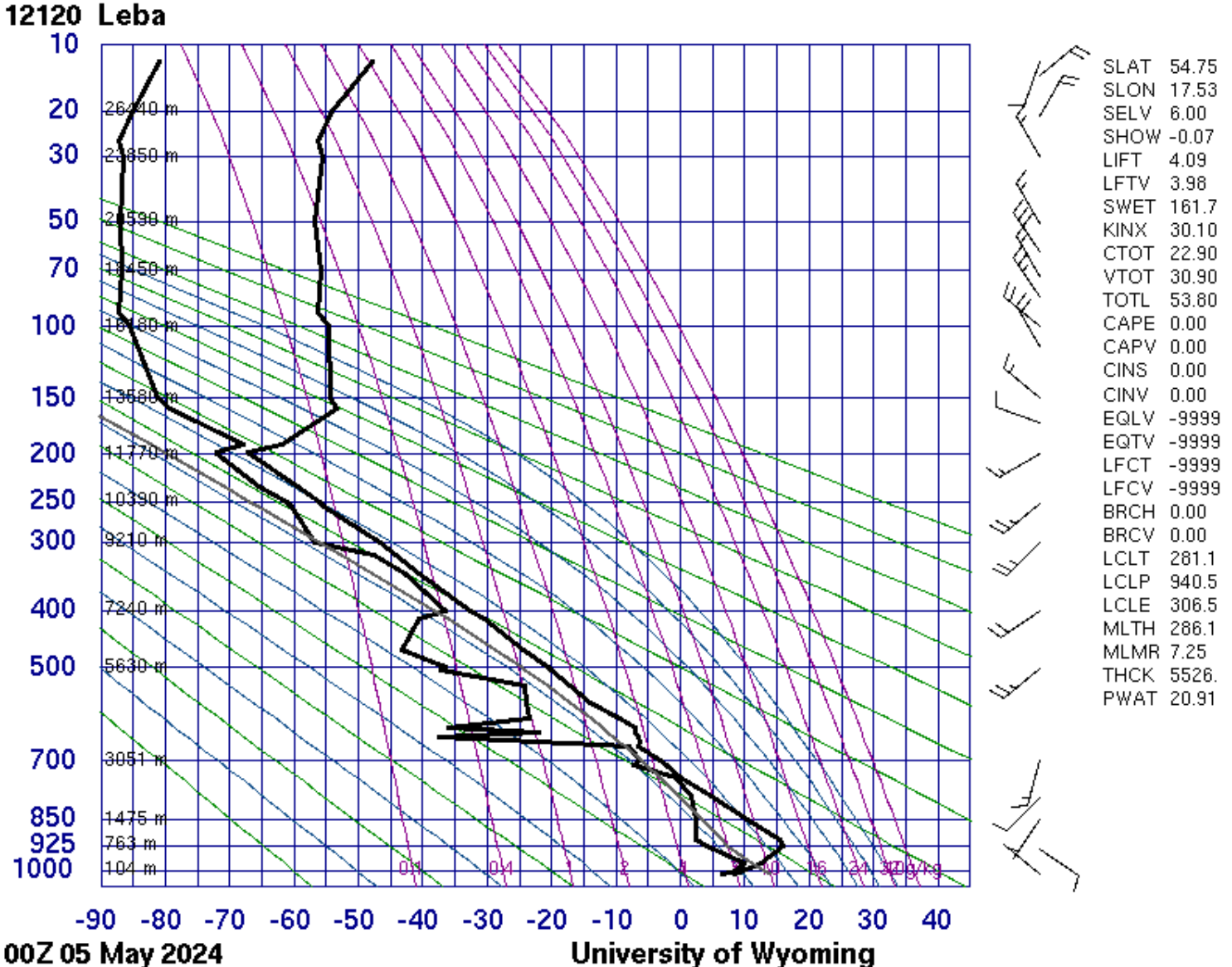
12120 Leba
10
20
30
50
70
100
150
200
250
300
400
500
700
850
925
1000
26440 m
23850 m
20590 m
18450 m
16180 m
13580 m
11770 m
10390 m
9210 m
7240 m
5630 m
3051 m
1475 m
763 m
104 m
-90 -80 -70 -60 -50 -40 -30 -20 -10 0 10 20 30 40
00Z 05 May 2024
University of Wyoming
SLAT 54.75
SLON 17.53
SELV 6.00
SHOW -0.07
LIFT 4.09
LFTV 3.98
SWET 161.7
KINX 30.10
CTOT 22.90
VTOT 30.90
TOTL 53.80
CAPE 0.00
CAPV 0.00
CINS 0.00
CINV 0.00
EQLV -9999
EQTV -9999
LFCT -9999
LFCV -9999
BRCH 0.00
BRCV 0.00
LCLT 281.1
LCLP 940.5
LCLE 306.5
MLTH 286.1
MLMR 7.25
THCK 5526.
PWAT 20.91

Primitive equations:

$$\frac{D\mathbf{V}}{Dt} + f\mathbf{k} \times \mathbf{V} = -\nabla\Phi$$

$$\frac{\partial \Phi}{\partial p} = -\alpha = -RT/p$$

$$\nabla \cdot \mathbf{V} + \frac{\partial \omega}{\partial p} = 0$$

$$\left(\frac{\partial}{\partial t} + \mathbf{V} \cdot \nabla\right) T + S_p \omega = J/c_p$$

S_p – stability parameter,
J – diabatic heating/cooling e.g. latent heat, divergence of radiative flux (absorption/emission)

..let's focus on vertical profiles

Thermal Equilibrium of the Atmosphere with a Convective Adjustment

SYUKURO MANABE AND ROBERT F. STRICKLER

General Circulation Research Laboratory, U. S. Weather Bureau, Washington, D. C.

(Manuscript received 19 December 1963, in revised form 13 April 1964)

1) Temporal development of temperature (stability) profile due to radiative fluxes

$$T^{\tau+1}=T^{\tau}+\left(\frac{\partial T}{\partial t}\right)^{\tau}\cdot\Delta t, \tag{1}$$

$$(\partial T/\partial z)^{\tau+1}=(\text{critical lapse rate}), \tag{2}$$

where

$$T^{\tau+1}=T^{\tau}+(\partial T/\partial t)_{\mathrm{NET}}{}^{\tau}\cdot\Delta t \tag{3}$$

and

$$\frac{C_p}{g}\int_{PcT}^{P*}\left(\frac{\partial T}{\partial t}\right)_{\mathrm{NET}}^{\tau}dp$$

$$=\frac{C_p}{g}\int_{PcT}^{P*}\left(\frac{\partial T}{\partial t}\right)_{\mathrm{RAD}}^{\tau}dp+(-F_0{}^{\tau}+S_0), \tag{4}$$

$$\frac{C_p}{g}\int_{P\,cT}^{P\,cB}\left(\frac{\partial T}{\partial t}\right)_{\mathrm{NET}}^{\tau}dp=\frac{C_p}{g}\int_{P\,cT}^{P\,cB}\left(\frac{\partial T}{\partial t}\right)_{\mathrm{RAD}}^{\tau}dp, \tag{5a}$$

Thermal Equilibrium of the Atmosphere with a Convective Adjustment

SYUKURO MANABE AND ROBERT F. STRICKLER

General Circulation Research Laboratory, U. S. Weather Bureau, Washington, D. C.

(Manuscript received 19 December 1963, in revised form 13 April 1964)

1) Temporal development of temperature (stability) profile due to radiative fluxes

2) „Convective adjustment" - added convective heat flux from the surface results in mean temperature gradient 6.5K/km in the troposphere.

$$\frac{C_p}{g}\int_{P_{cT}}^{P_{cB}}\left(\frac{\partial T}{\partial t}\right)_{\text{NET}}^{\tau} dp=\frac{C_p}{g}\int_{P_{cT}}^{P_{cB}}\left(\frac{\partial T}{\partial t}\right)_{\text{RAD}}^{\tau} dp, \quad (5a)$$

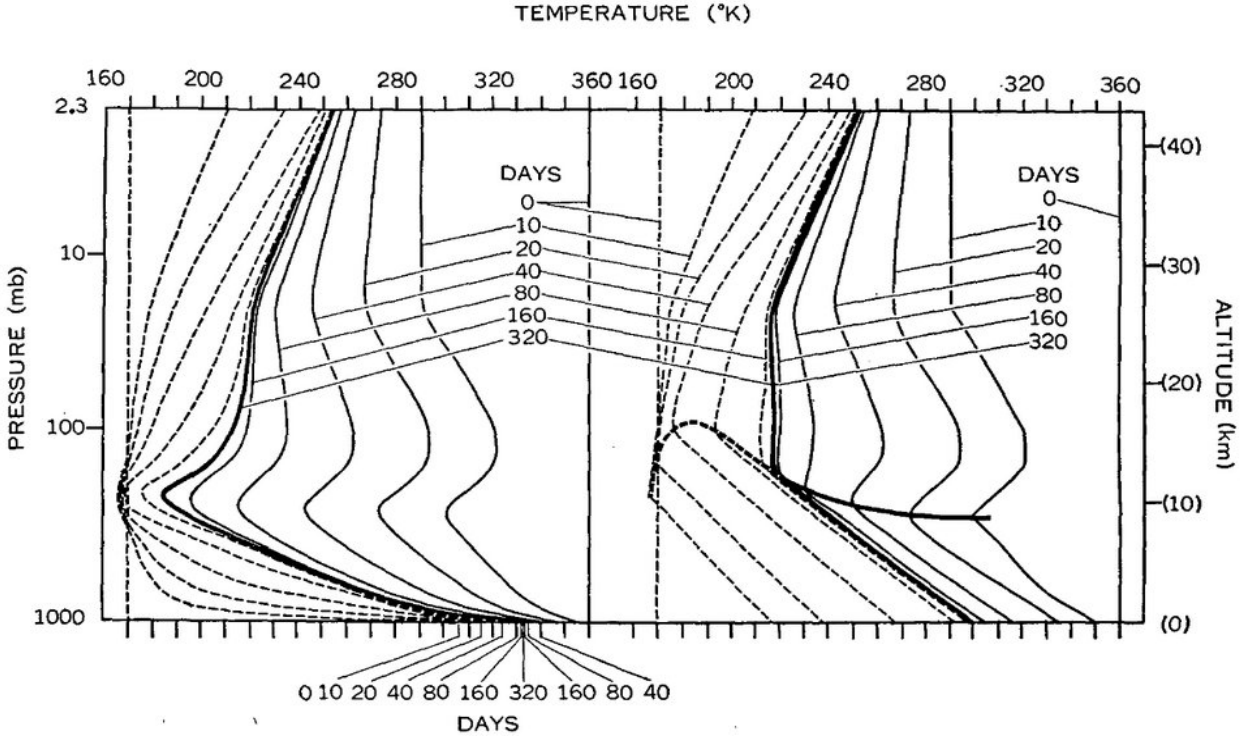

FIG. 1. The left and right hand sides of the figure, respectively, show the approach to states of pure radiative and thermal equilibrium. The solid and dashed lines show the approach from a warm and cold isothermal atmosphere.

1) Temporal development of temperature (stability) profile due to radiative fluxes

2) „Convective adjustment” - added convective heat flux from the surface results in mean temperature gradient 6.5K/km in the troposphere.

3) Effects of clouds on longwave and shortwave radiation added.

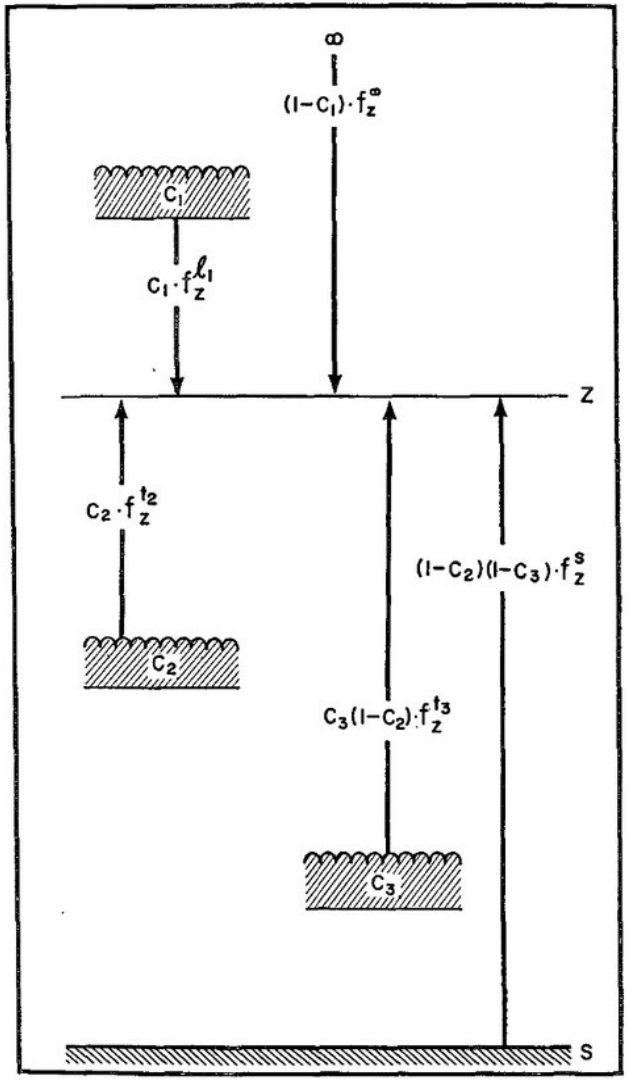

FIG. 2. Long wave radiation in an atmosphere with clouds.

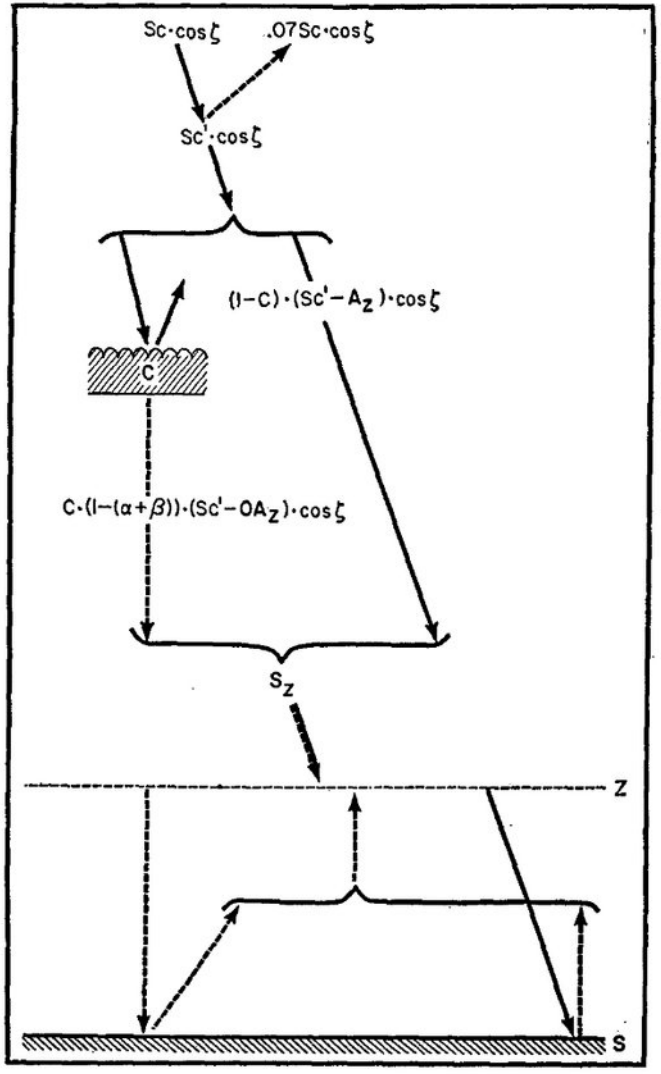

FIG. 3. Vertical distribution of the flux of solar radiation in an atmosphere with clouds.

1) Temporal development of temperature (stability) profile due to radiative fluxes

2) „Convective adjustment” - added convective heat flux from the surface results in mean temperature gradient 6.5K/km in the troposphere.

3) Effects of clouds on longwave and shortwave radiation added.

4) Adjustment for the effects of observed vertical profiles of main GHG’s.

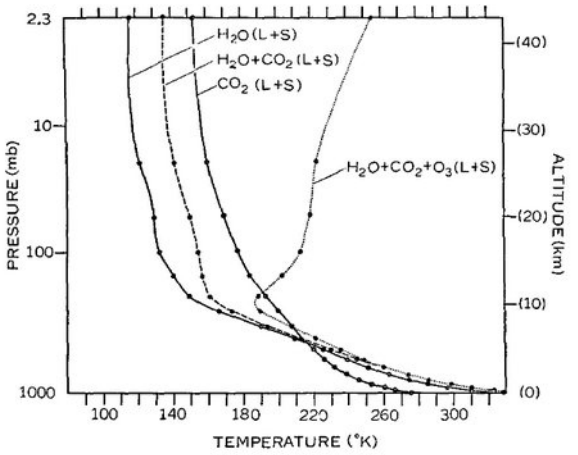

FIG. 6a. Pure radiative equilibrium for various atmospheric absorbers. The distribution of gaseous absorbers at 35N in April are used. $S_e=2$ ly min^{-1}, $\cos\bar{\zeta}=0.5$, $r=0.5$. No clouds. (L+S) means that the effects of both long wave radiation and solar radiation are included.

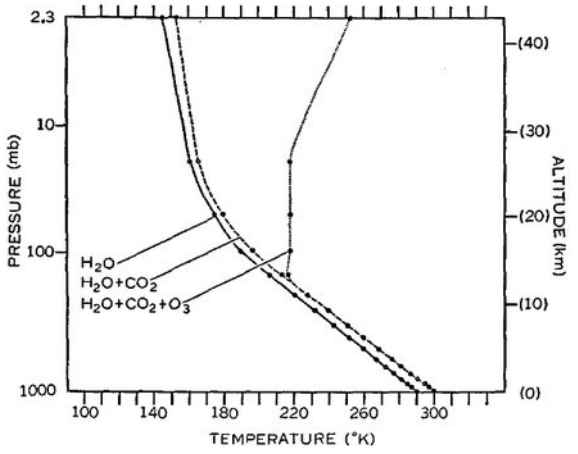

FIG. 6c. Thermal equilibrium of various atmospheres which have a critical lapse rate of 6.5 deg km^{-1}. Vertical distributions of gaseous absorbers at 35N, April, were used. $S_e=2$ ly min^{-1}, $\cos\bar{\zeta}=0.5$, $r=0.5$, no clouds.

Thermal Equilibrium of the Atmosphere with a Given Distribution of Relative Humidity

SYUKURO MANABE AND RICHARD T. WETHERALD

Geophysical Fluid Dynamics Laboratory, ESSA, Washington, D. C.

(Manuscript received 2 November 1966)

ABSTRACT

Radiative convective equilibrium of the atmosphere with a given distribution of relative humidity is computed as the asymptotic state of an initial value problem.

The results show that it takes almost twice as long to reach the state of radiative convective equilibrinm for the atmosphere with a given distribution of relative humidity than for the atmosphere with a given distribution of absolute humidity.

Also, the surface equilibrium temperature of the former is almost twice as sensitive to change of various factors such as solar constant, CO_2 content, O_3 content, and cloudiness, than that of the latter, due to the adjustment of water vapor content to the temperature variation of the atmosphere.

According to our estimate, a doubling of the CO_2 content in the atmosphere has the effect of raising the temperature of the atmosphere (whose relative humidity is fixed) by about 2C. Our model does not have the extreme sensitivity of atmospheric temperature to changes of CO_2 content which was adduced by Möller.

TABLE 4. Equilibrium temperature of the earth's surface (°K) and the CO_2 content of the atmosphere.

CO_2 content (ppm)	Average cloudiness		Clear	
	Fixed absolute humidity	Fixed relative humidity	Fixed absolute humidity	Fixed relative humidity
150	289.80	286.11	298.75	304.40
300	291.05	288.39	300.05	307.20
600	292.38	290.75	301.41	310.12

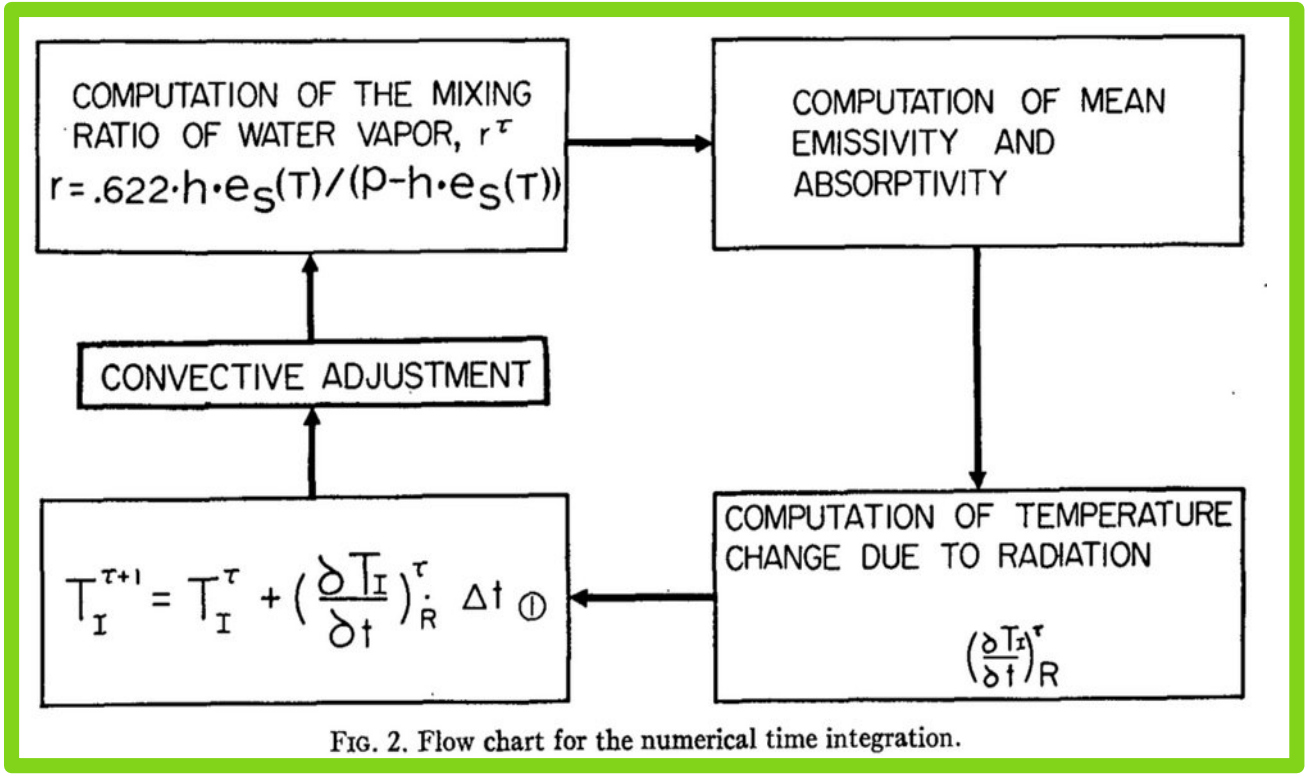

FIG. 2. Flow chart for the numerical time integration.

Carbon dioxide heats the atmosphere

Increased levels of carbon dioxide lead to higher temperatures in the lower atmosphere, while the upper atmosphere gets colder. Manabe thus confirmed that the variation in temperature is due to increased levels of carbon dioxide; if it was caused by increased solar radiation, the entire atmosphere should have warmed up.

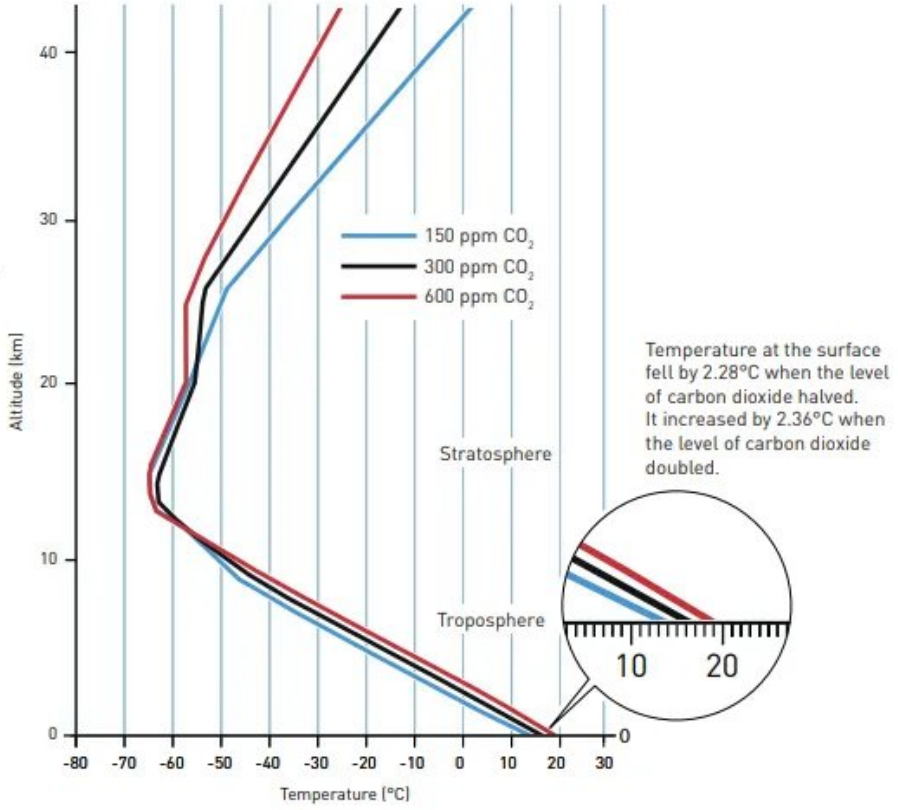

Temperature at the surface fell by 2.28°C when the level of carbon dioxide halved. It increased by 2.36°C when the level of carbon dioxide doubled.

Source: Manabe and Wetherald (1967) Thermal equilibrium of the atmosphere with a given distribution of relative humidity, *Journal of the atmospheric sciences*, Vol. 24, Nr 3, May.

How to account for convection?

TABLE 4. Equilibrium temperature of the earth's surface (°K) and the CO_2 content of the atmosphere.

CO_2 content (ppm)	Average cloudiness		Clear	
	Fixed absolute humidity	Fixed relative humidity	Fixed absolute humidity	Fixed relative humidity
150	289.80	286.11	298.75	304.40
300	291.05	288.39	300.05	307.20
600	292.38	290.75	301.41	310.12

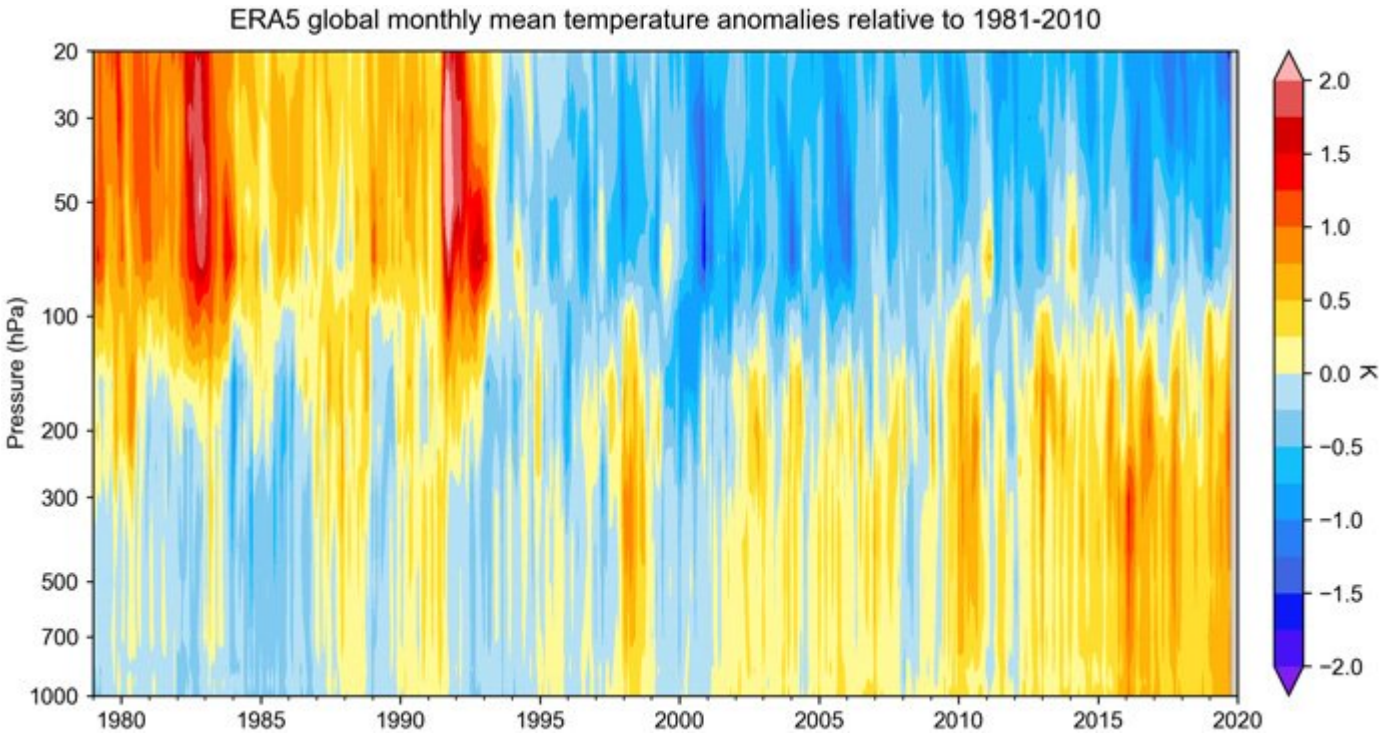

https://www.ecmwf.int/en/research/climate-reanalysis

Cloud Feedback Processes in a General Circulation Model

R. T. WETHERALD AND S. MANABE

Geophysical Fluid Dynamics Laboratory/NOAA, Princeton University, Princeton, New Jersey

(Manuscript received 6 April 1987, in final form 30 November 1987)

ABSTRACT

The influence of the cloud feedback process upon the sensitivity of climate is investigated by comparing the behavior of two versions of a climate model with predicted and prescribed cloud cover. The model used for this study is a general circulation model of the atmosphere coupled with a mixed layer model of the oceans. The sensitivity of each version of the model is inferred from the equilibrium response of the model to a doubling of the atmospheric concentration of carbon dioxide.

It is found that the cloud feedback process in the present model enhances the sensitivity of the model climate. In response to the increase of atmospheric carbon dioxide, cloudiness increases around the tropopause and is reduced in the upper troposphere, thereby raising the height of the cloud layer in the upper troposphere. This rise of the high cloud layer implies a reduction of the temperature of the cloud top and, accordingly, of the upward terrestrial radiation from the top of the model atmosphere. Thus, the heat loss from the atmosphere–earth system of the model is reduced. As the high cloud layer rises, the vertical distribution of cloudiness changes, thereby affecting the absorption of solar radiation by the model atmosphere. At most latitudes the effect of reduced cloud amount in the upper troposphere overshadows that of increased cloudiness around the tropopause, thereby lowering the global mean planetary albedo and enhancing the CO_2 induced warming.

On the other hand, the increase of low cloudiness in high latitudes raises the planetary albedo and thus decreases the CO_2 induced warming of climate. However, the contribution of this negative feedback process is much smaller than the effect of the positive feedback process involving the change of high cloud.

The model used here does not take into consideration the possible change in the optical properties of clouds due to the change of their liquid water content. In view of the extreme idealization in the formulation of the cloud feedback process in the model, this study should be regarded as a study of the mechanisms involved in this process rather than the quantitative assessment of its influence on the sensitivity of climate.

Interaction of a Cumulus Cloud Ensemble with the Large-Scale Environment, Part I

AKIO ARAKAWA AND WAYNE HOWARD SCHUBERT[1]

Dept. of Meteorology, University of California, Los Angeles 90024

(Manuscript received 10 August 1973, in revised form 7 November 1973)

ABSTRACT

A theory of the interaction of a cumulus cloud ensemble with the large-scale environment is developed. In this theory, the large-scale environment is divided into the subcloud mixed layer and the region above. The time changes of the environment are governed by the heat and moisture budget equations for the subcloud mixed layer and for the region above, and by a prognostic equation for the depth of the mixed layer. In the environment above the mixed layer, the cumulus convection affects the temperature and moisture fields through cumulus-induced subsidence and detrainment of saturated air containing liquid water which evaporates in the environment. In the subcloud mixed layer, the cumulus convection does not act directly on the temperature and moisture fields, but it affects the depth of the mixed layer through cumulus-induced subsidence. Under these conditions, the problem of parameterization of cumulus convection reduces to the determination of the vertical distributions of the total vertical mass flux by the ensemble, the total detrainment of mass from the ensemble, and the thermodynamical properties of the detraining air.

The cumulus ensemble is spectrally divided into sub-ensembles according to the fractional entrainment rate, given by the ratio of the entrainment per unit height to the vertical mass flux in the cloud. For these sub-ensembles, the budget equations for mass, moist static energy, and total water content are obtained. The solutions of these equations give the temperature excess, the water vapor excess, and the liquid water content of each sub-ensemble, and further reduce the problem of parameterization to the determination of the mass flux distribution function, which is the sub-ensemble vertical mass flux at the top of the mixed layer.

The cloud work function, which is an integral measure of the buoyancy force in the clouds, is defined for each sub-ensemble; and, under the assumption that it is in quasi-equilibrium, an integral equation for the mass flux distribution function is derived. This equation describes how a cumulus ensemble is forced by large-scale advection, radiation, and surface turbulent fluxes, and it provides a closed parameterization of cumulus convection for use in prognostic models of large-scale atmospheric motion.

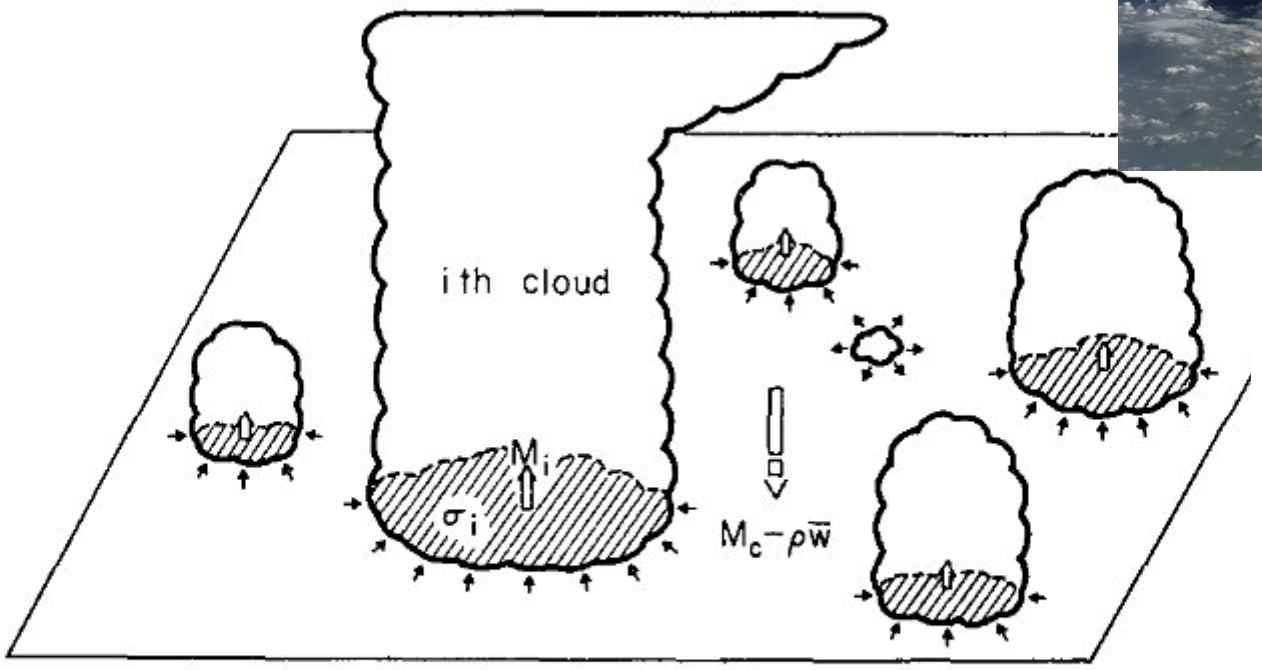

FIG. 1. A unit horizontal area at some level between cloud base and the highest cloud top. The taller clouds are shown penetrating this level and entraining environmental air. A cloud which has lost buoyancy is shown detraining cloud air into the environment.

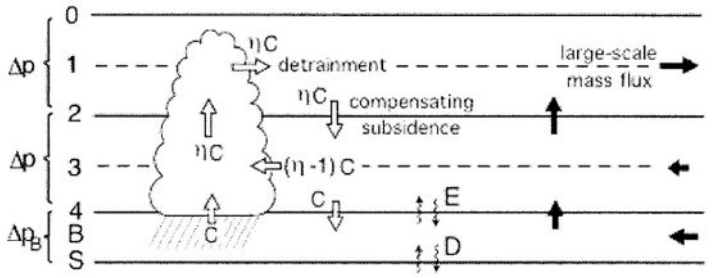

FIG. 6. One of the three cloud types considered in Arakawa's (1969) parameterization for a three-level model. Solid and open arrows show large-scale and superposed cumulus-induced mass fluxes, respectively.

Formulation structure of the mass-flux convection parameterization

Jun-Ichi Yano*

CNRM, Météo-France and CNRS, 31057 Toulouse Cedex, France

ARTICLE INFO

Article history:
Received 2 November 2013
Received in revised form 22 April 2014
Accepted 30 April 2014
Available online 13 May 2014

Keywords:
Parameterization
Convection
Subgr-scale processes
Mass flux

ABSTRACT

Structure of the mass-flux convection parameterization formulation is re-examined. Many of the equations associated with this formulation are derived in systematic manner with various intermediate steps explicitly presented. The nonhydrostatic anelastic model (NAM) is taken as a starting point of all the derivations.

Segmentally constant approximation (SCA) is a basic geometrical constraint imposed on a full system (e.g., NAM) as a first step for deriving the mass-flux formulation. The standard mass-flux convection parameterization, as originally formulated by Ooyama, Fraedrich, Arakawa and Schubert, is re-derived under the two additional hypotheses concerning entrainment–detrainment and environment, and an asymptotic limit of vanishing areas occupied by convection.

A model derived at each step of the deduction constitutes a stand-alone subgrid-scale representation by itself, leading to a hierarchy of subgrid-scale schemes. A backward tracing of this deduction process provides paths for generalizing mass-flux convection parameterization. Issues of the high-resolution limit for parameterization are also understood as those of relaxing various traditional constraints. The generalization presented herein can include various other subgrid-scale processes under a mass-flux framework.

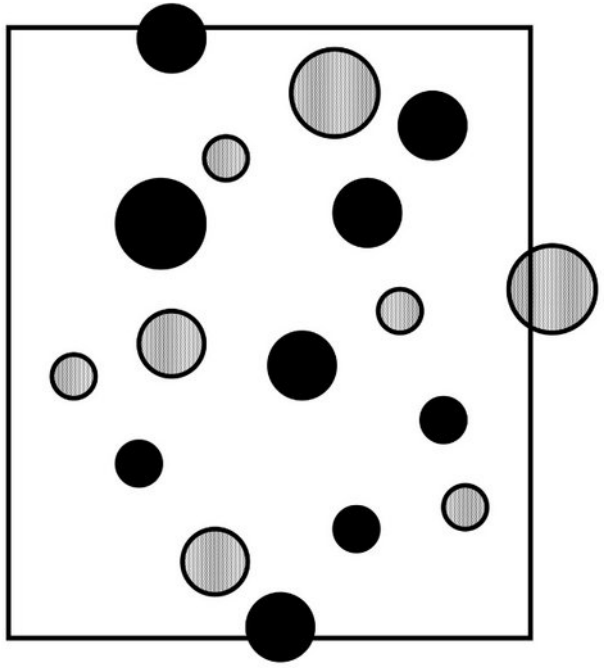

Fig. 2. A generalization of Riehl and Malkus' hot-tower hypothesis in Fig. 1 into two convective-scale components: dark circles and gray circles representing updrafts and downdrafts, respectively. This corresponds to a special case of segmentally-constant approximation (SCA) over subgrid-scale processes.

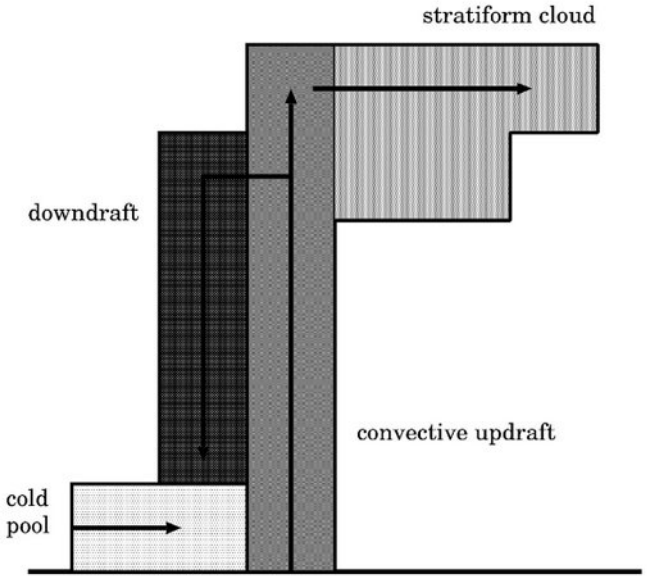

Fig. 3. A side view for a further generalization of SCA. Unlike the case of Fig. 2, the subgrid-scale components are no longer exclusively interacting with the environment, but with various other components: convective updraft, downdraft, cold pool, stratiform cloud.

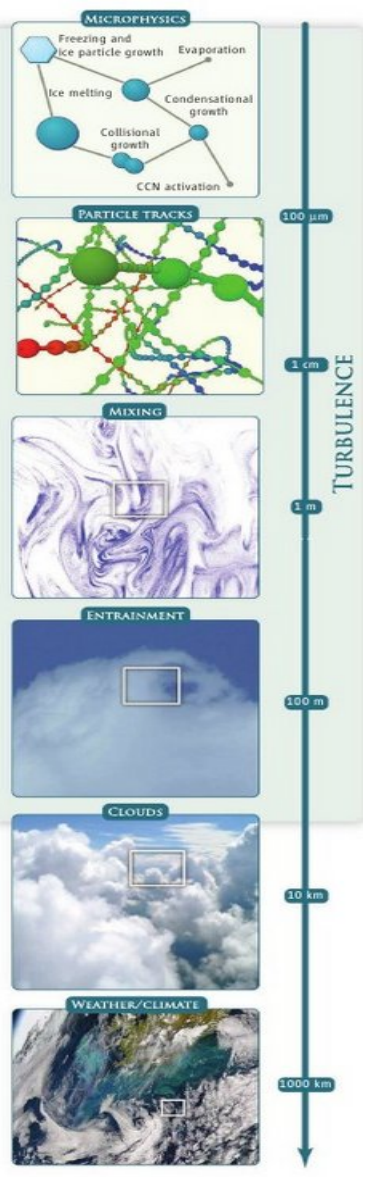

Cloud process parameterizations: „Multiscale modeling”, superparametrizations, explicit cloud-resolving, GIGA-LES, ILES,

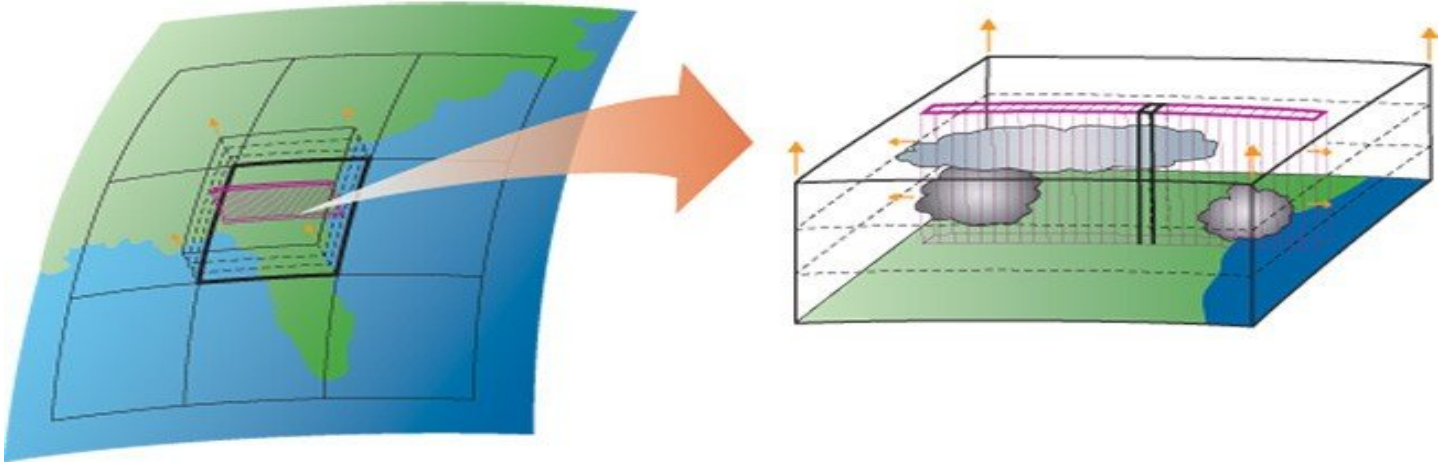

Bodenschatz, E., S.P. Malinowski, R.A. Shaw, F. Stratmann, 2010: Can We Understand Clouds without Turbulence? *Science,* **327**, 970 – 971.

Randall D.A, Khairoutdinov M, Arakawa A, Grabowski W.W., 2003: Breaking the cloud parameterization deadlock . Bull. Amer. Meteorol. Soc., **84**, 1547-1564.

I wiele wiele innych.....

On a level of gridboxes:

Smagorinsky-Lilly Subgrid Scale Model

The Smagorinsky-Lilly SGS model is based on the Prandtl's mixing length model and assumes that a kinematic SGS viscosity can be expressed in terms of the length scale and the strain rate magnitude of the resolved flow.

$$\tau'_{ij} = \rho\widetilde{u_i u_j} - \rho\widetilde{u_i}\widetilde{u_j} = -2\mu_s\widetilde{S_{ij}}$$

(1

where

- $\mu_s = \rho(C_S\Delta)^2\sqrt{2\widetilde{S_{ij}}\widetilde{S_{ij}}}$ is the subgrid turbulent viscosity,
- Model constant 0.17 < C_s < 0.21 (Lilly, 1996)
- $\widetilde{S_{ij}} = \frac{1}{2}\left(\frac{\partial\widetilde{u_i}}{\partial x_j} + \frac{\partial\widetilde{u_j}}{\partial x_i}\right)$ is the filtered (resolved) strain rate tensor

A major drawback of this model is that the model constant (C_s) does not vary in space and time. Furthermore, this model has no correct wall behavior and it is too dissipative for laminar turbulent transition cases. These limitations led to the development of a dynamic model for which the model constant is allowed to vary depending on the grid resolution and flow regime.

For anisotropic grid:

$\Delta = (\Delta x\ \Delta y\ \Delta z)^{1/3}$

…… many variations

https://help.altair.com/hwcfdsolvers/acusolve/topics/acusolve/training_manual/smagorinksy_lilly_subgrid_scale_model_r.htm

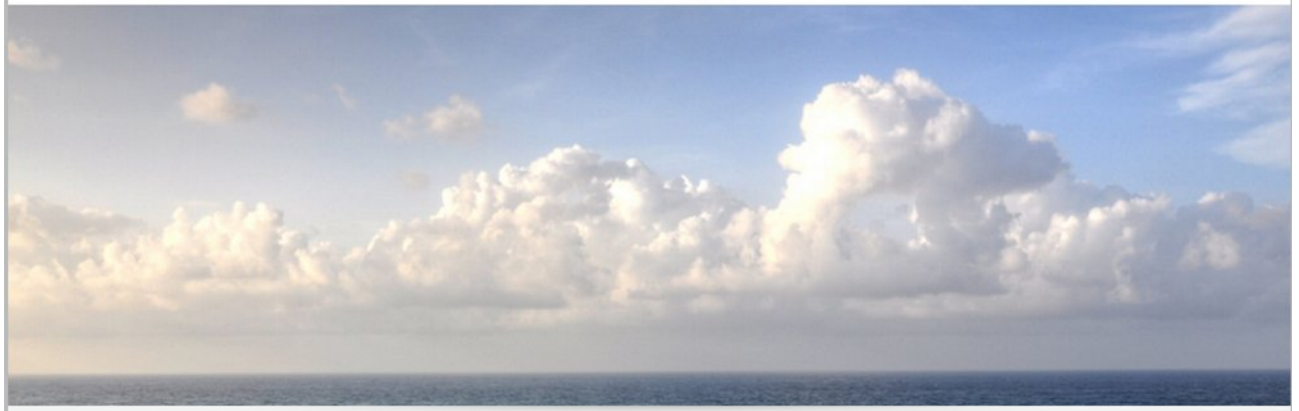

RCEMIP: Radiative-Convective Equilbrium Model Intercomparison Project

RCEMIP-II

We are excited to move towards a Phase II of RCEMIP, which will involve simulations with a prescribed analytic SST boundary condition. For more info check out: RCEMIP Simulations and the RCEMIP-II protocol paper. **Registration for participating in Phase II is now open!**

Click here for Archived Updates

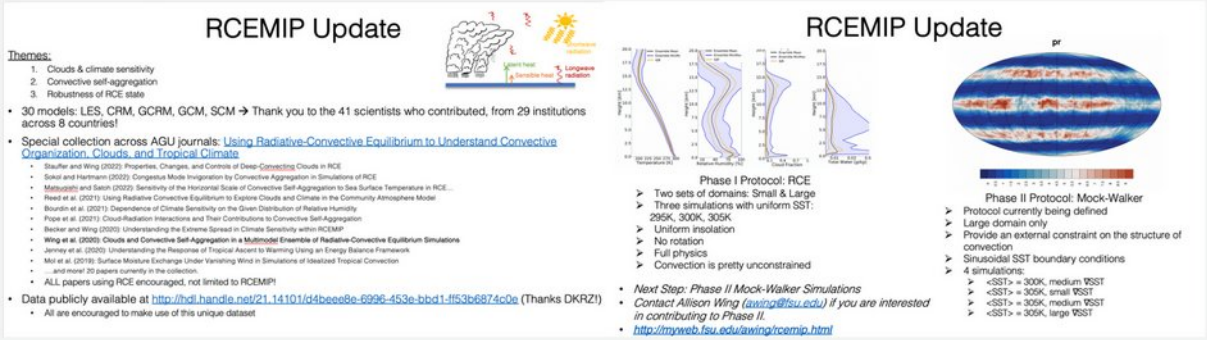

SUMMARY:

Despite some robust behaviors, there is substantial disagreement across the RCEMIP ensemble in representations of cloudiness, self-aggregation, and climate sensitivity. Some readers may find this discouraging or surprising (perhaps hoping that models with explicit convection might have agreed better), while some readers may have anticipated that the many degrees of freedom in how models may achieve RCE would result in divergent behavior.

Indeed, because RCE is relatively unconstrained, with convection left free to evolve as long as energy balance is still met, it is a tough test for models. We argue that this is a benefit of RCE, rather than a weakness. The divergent behavior in RCEMIP reveals the true sensitivities to representations of convection, microphysics, turbulence, and dynamical cores, sensitivities that might be masked in other comparisons by constraints imposed by large-scale circulations.
Furthermore, the **RCEMIP results show that the wide range of equilibrated states is not due to differences in the basic configuration such as SST, CRM grid spacing, insolation, or initialization**, as there is a large spread despite constraining these factors to be the same. **Instead, the different responses must be due to differences in model physics and/or numerics.**

Diurnal organization of convection, strong heat fluxes:
Two realistic anelastic simulations of cumulus convection over Poland, ~1km grid, two different advection schemes.

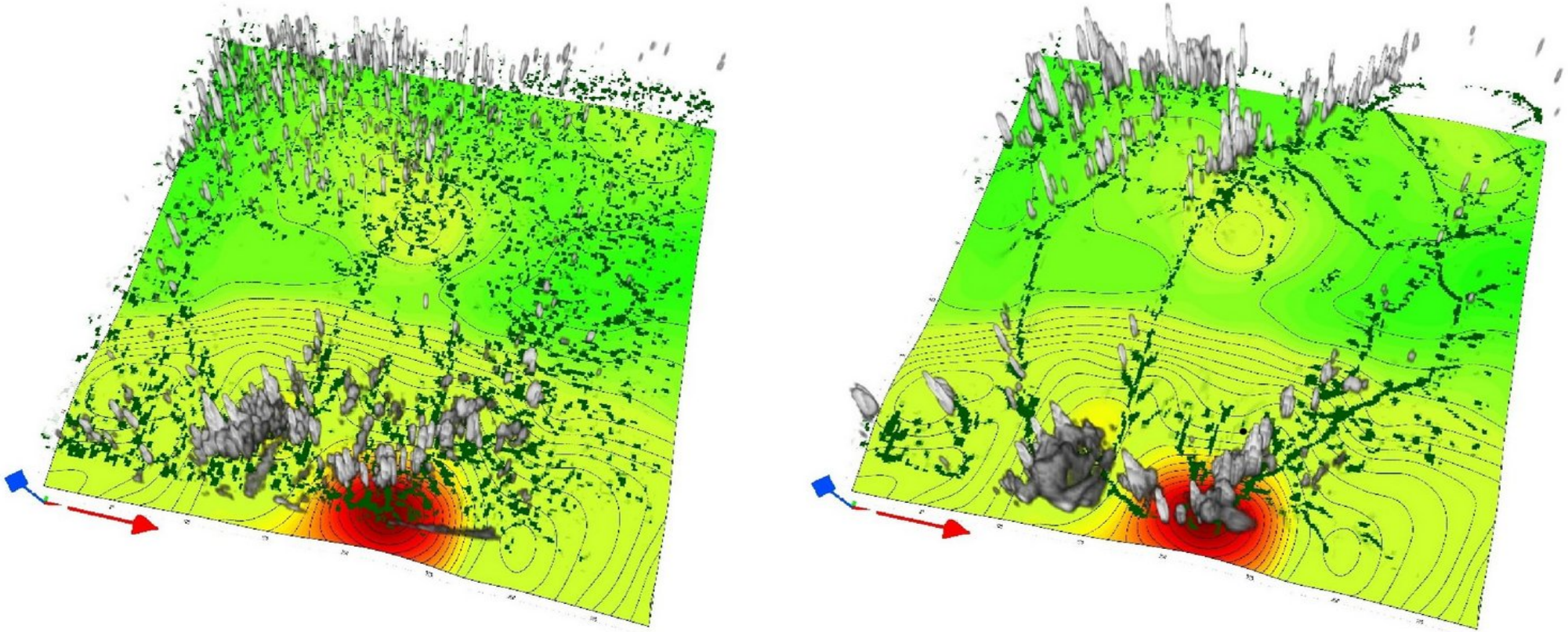

Piotrowski, Z.P., Smolarkiewicz, P.K, Malinowski, S.P., Wyszogrodzki A.A., 2009, On numerical realizability of thermal convection, Journal of Computational Physics, vol. 228, 6268-6290, 10.1016/j.jcp.2009.05.023

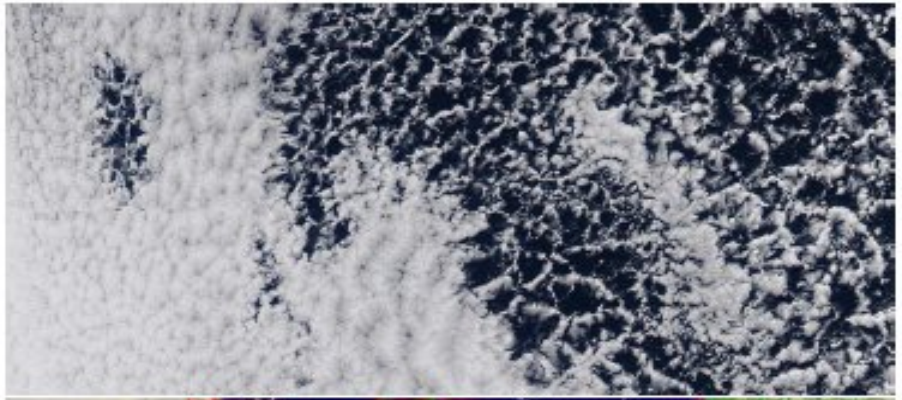

Similar or
not ?

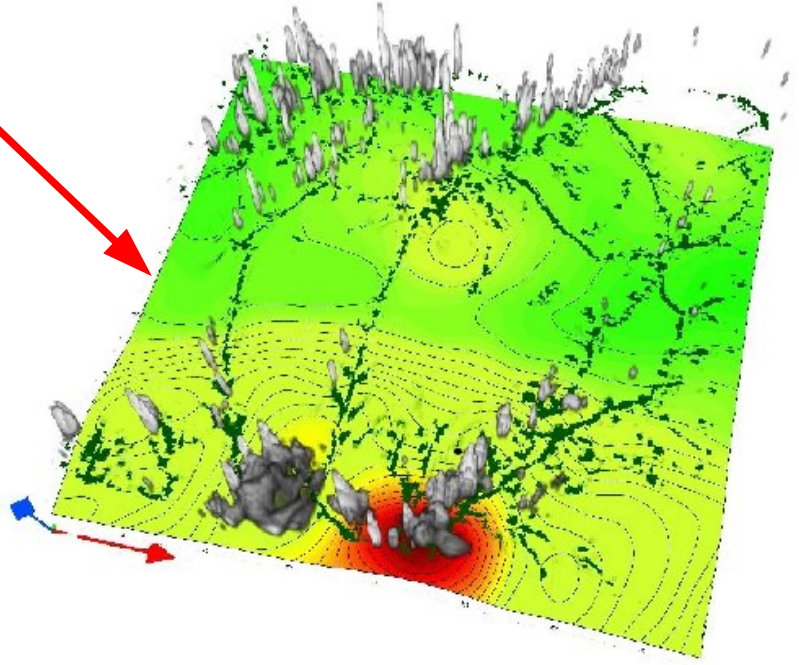

Rayleigh number :

$$Ra = \frac{g\Delta\overline{\theta}h^3}{\overline{\theta}\nu\nu_\theta}$$

g – gravity acceleration
h – fluid depth
ν – kinematic viscosity
ν_θ – thermal diffusivity
$\Delta\theta/\theta$ – relative change of stability

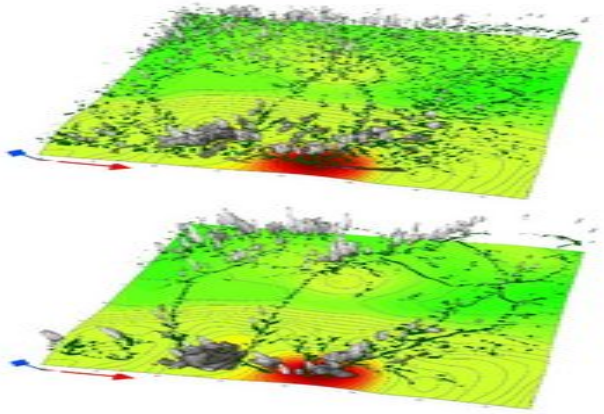

>> critical

rigid/free boundary

Ra_c=1100.657

>~ critical

In the atmosphere Ra ≈ O(10^{16})

How to explain convective patterns ?

$$Ra = \frac{g\Delta\overline{\theta}h^3}{\overline{\theta}K_m^2}$$

Effective eddy diffusivity

Notice that K_m in vertical and horizontal may differ, e.g. due to grid anisotropy.

Idealized simulation, no wind, constant viscosities

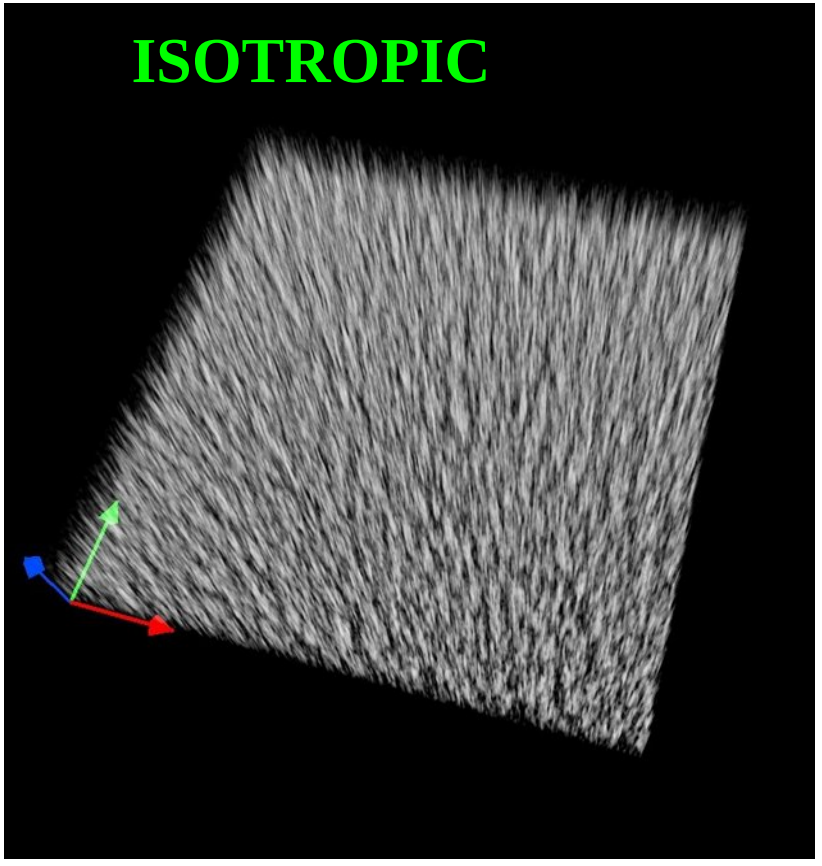

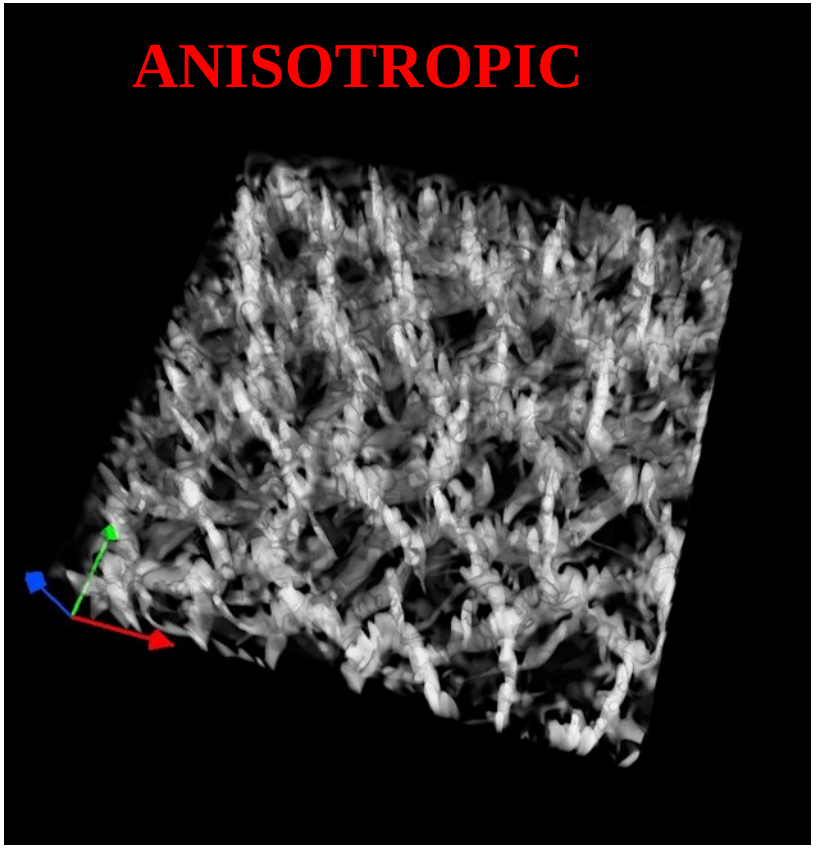

The only difference – horizontal viscosity,

$\nu_h = 2.5\ m^2 s^{-1}$ vs. $\nu_h = 70\ m^2 s^{-1}$; vertical $\nu_v = 2.5\ m^2 s^{-1}$

Requirements to simulate convective fields

- Numerical viscosity control - not all dissipative numerics have the right properties needed for ILES simulations
- Awareness of the design of the numerical model - avoiding dissipative first-order schemes and filters
- Verification of subscale schemes for their suitability to a particular problem
- Skepticism for attractive convection structures and cloud fields in large nonhydrostatic simulations Cellular convection in meso and large-scale models can only be a messy effect of anisotropic viscosity

On a level of gridboxes:

Smagorinsky-Lilly Subgrid Scale Model

The Smagorinsky-Lilly SGS model is based on the Prandtl's mixing length model and assumes that a kinematic SGS viscosity can be expressed in terms of the length scale and the strain rate magnitude of the resolved flow.

$$\tau'_{ij} = \rho\widetilde{u_i u_j} - \rho\widetilde{u_i}\widetilde{u_j} = -2\mu_s\widetilde{S_{ij}}$$

(1

where

- $\mu_s = \rho(C_S\Delta)^2\sqrt{2\widetilde{S_{ij}}\widetilde{S_{ij}}}$ is the subgrid turbulent viscosity,
- Model constant 0.17 < C_s < 0.21 (Lilly, 1996)
- $\widetilde{S_{ij}} = \frac{1}{2}\left(\frac{\partial\widetilde{u_i}}{\partial x_j} + \frac{\partial\widetilde{u_j}}{\partial x_i}\right)$ is the filtered (resolved) strain rate tensor

A major drawback of this model is that the model constant (C_s) does not vary in space and time. Furthermore, this model has no correct wall behavior and it is too dissipative for laminar turbulent transition cases. These limitations led to the development of a dynamic model for which the model constant is allowed to vary depending on the grid resolution and flow regime.

For anisotropic grid:

$\Delta = (\Delta x\ \Delta y\ \Delta z)^{1/3}$

…… many variations

https://help.altair.com/hwcfdsolvers/acusolve/topics/acusolve/training_manual/smagorinksy_lilly_subgrid_scale_model_r.htm

SOME PRACTICE – MY EXPERIENCE WITH ATMOSPHERIC tURBULENCE

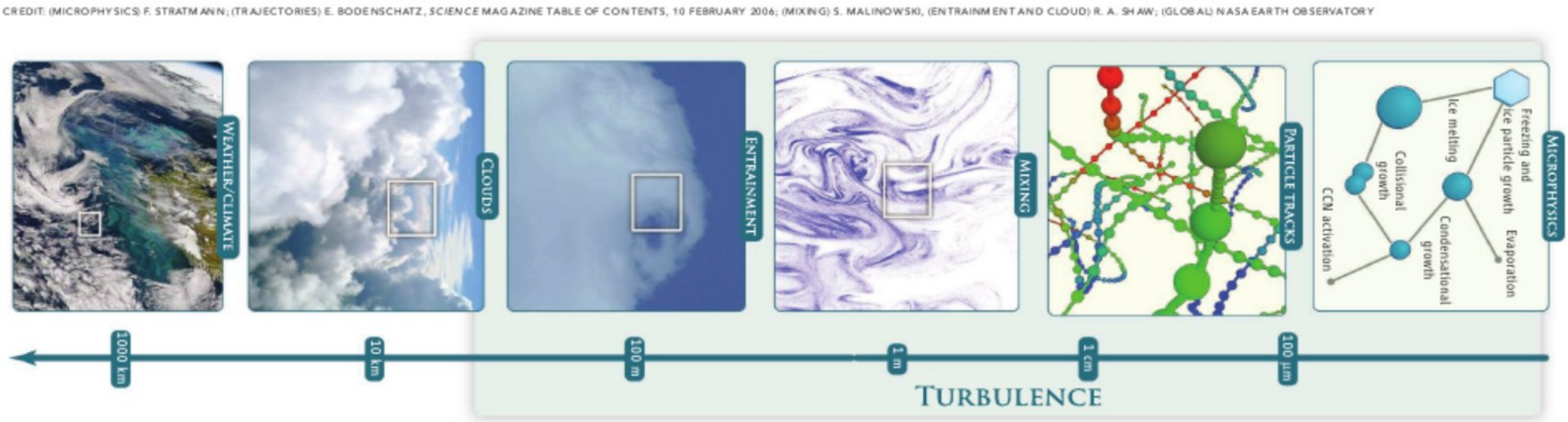

Coming to smaller scales you find, that the situation is not less complicated… Clouds, cloud particles. Phase changes occur in microscales, yet they affect larger scales. Radiation effects of clouds and aerosols are also important.

Bodenschatz, Malinowski, Shaw, Stratmann.,
„Can we understand clouds without turbulence?" Science, 2010.

We will consider mostly turbulence measured by means of airborne instrumentation, mostly in the course of three research campaigns:

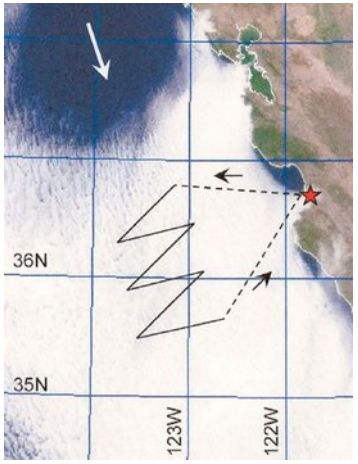

POST (2008)

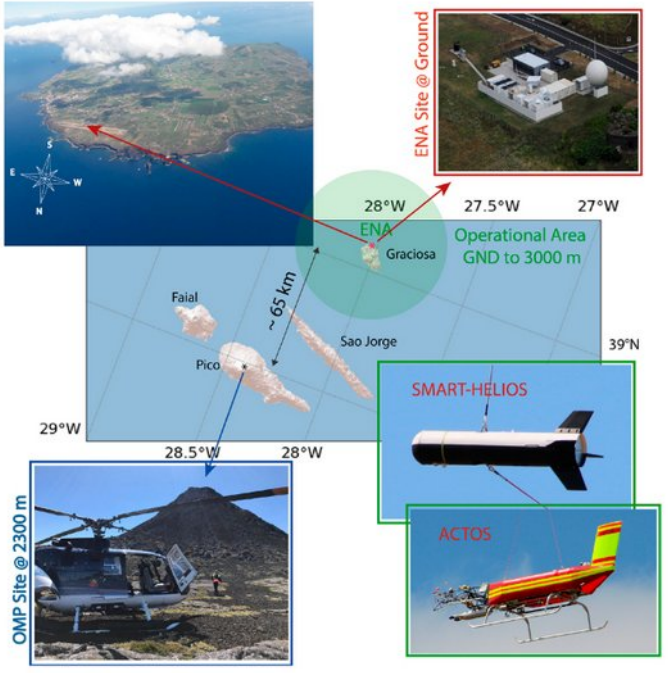

ACORES(2017)

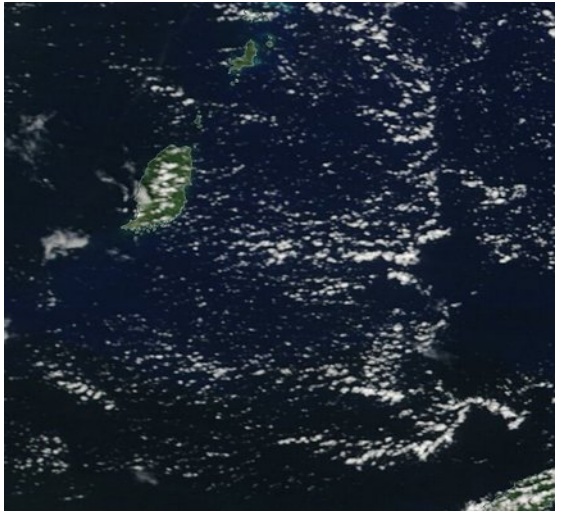

EUREC4A(2020)

Physics of stratocumulus top POST

Physics of
Stratocumulus
Tops
Flight 10
08/04/2008

Date	2008-08-04
UTC	18:26:43
GLAT	36.5821
GLON	123.6621
GALT	769.1
RADALT	954.9
TAS	60
THDG	062
PITCH	2
ROLL	0
PS	926.5
AT	18.2
SST	8.7
RHUM	27
WDC	341
WSC	6.2
WVC	0.3
LWC3	0.00
CONC_CPCI	1070
CONC_CAS	0.0
CONC_CIP	0.000
GGDSP	59.0

POST flight strategy:

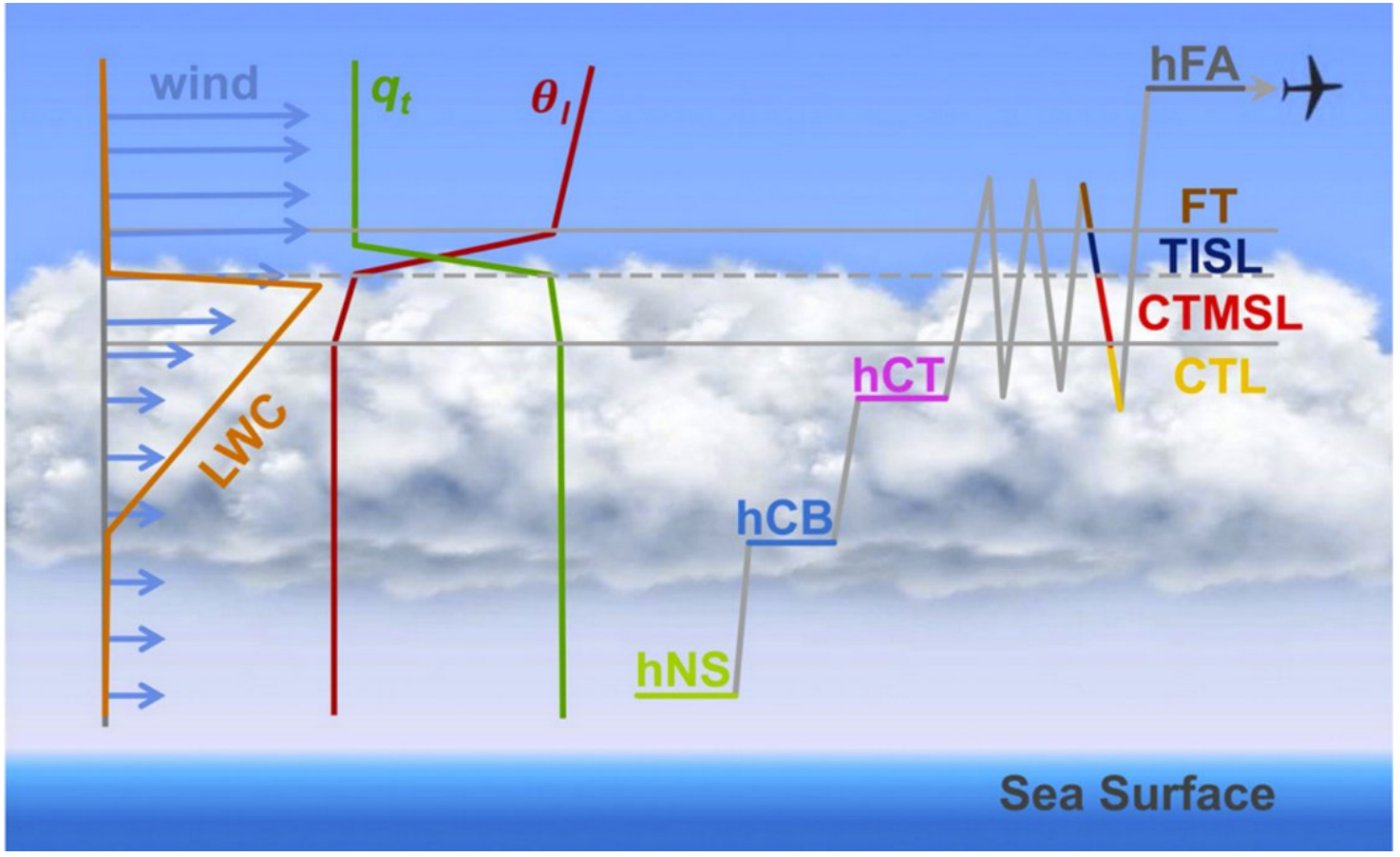

Gerber, H.,et al., 2013: Entrainment rates and microphysics in POST stratocumulus, J. Geophys. Res. Atmos., 118, 12,094–12,109.

“TYPICAL” (TO10)

“NON-TYPICAL” (TO13)

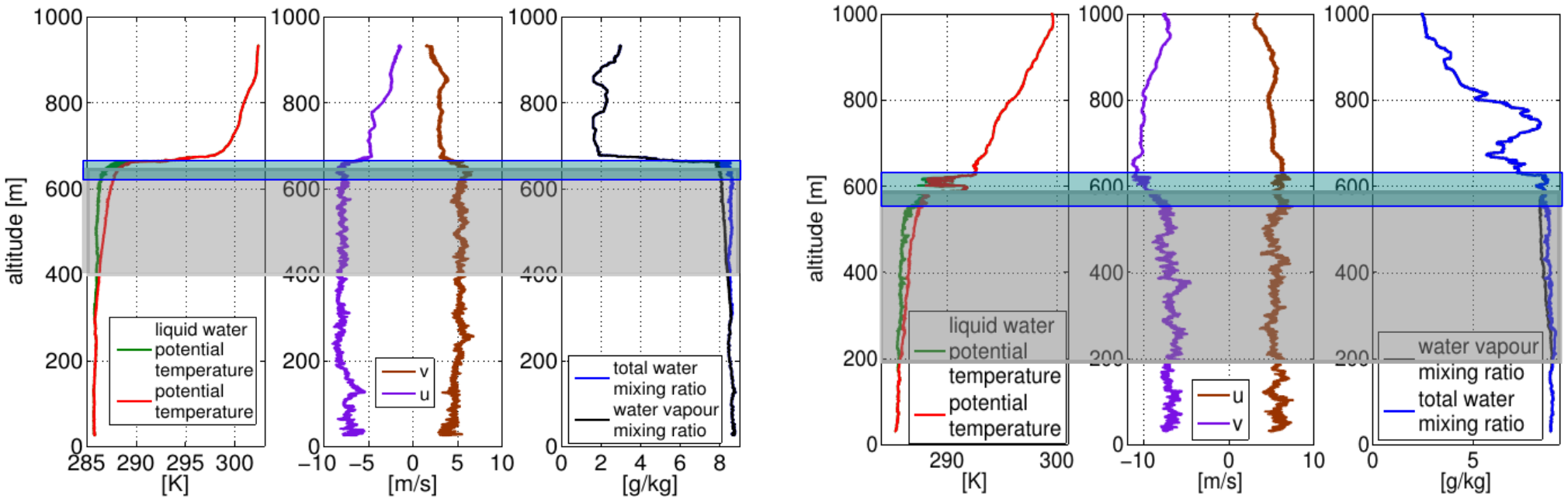

Example profiles of temperature, wind and humidity across the Stratocumulus Topped Boundary Layer.
grey shading: cloud, blue shading: EIL=TISL+CTMSL

Malinowski, S. P. et al., 2013: Physics of Stratocumulus Top (POST): Turbulent mixing across capping inversion. Atmos. Chem. Phys., 13, 15 233–269.

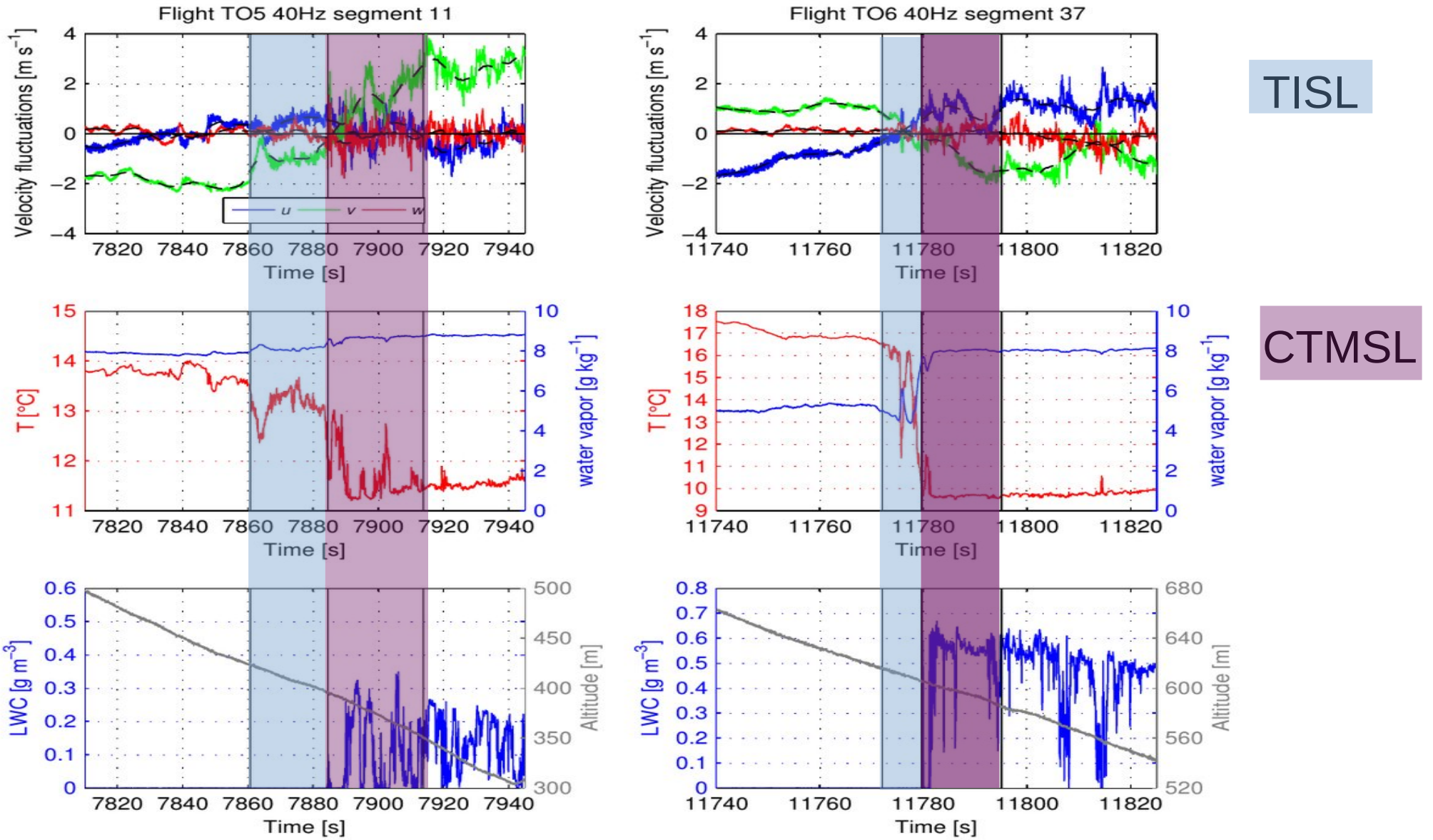
Flight TO5 40Hz segment 11
Flight TO6 40Hz segment 37
Velocity fluctuations [m s^{-1}]
u
v
w
Time [s]
T [°C]
water vapor [g kg^{-1}]
LWC [g m^{-3}]
Altitude [m]
TISL
CTMSL

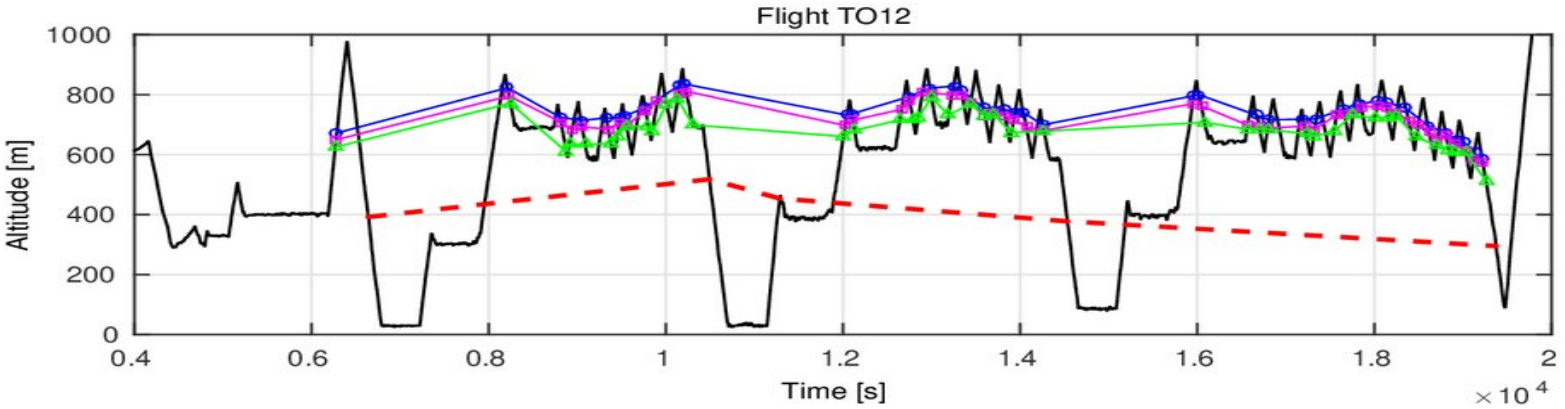

Algorithmic layer division allows for objective characterization of the layers.

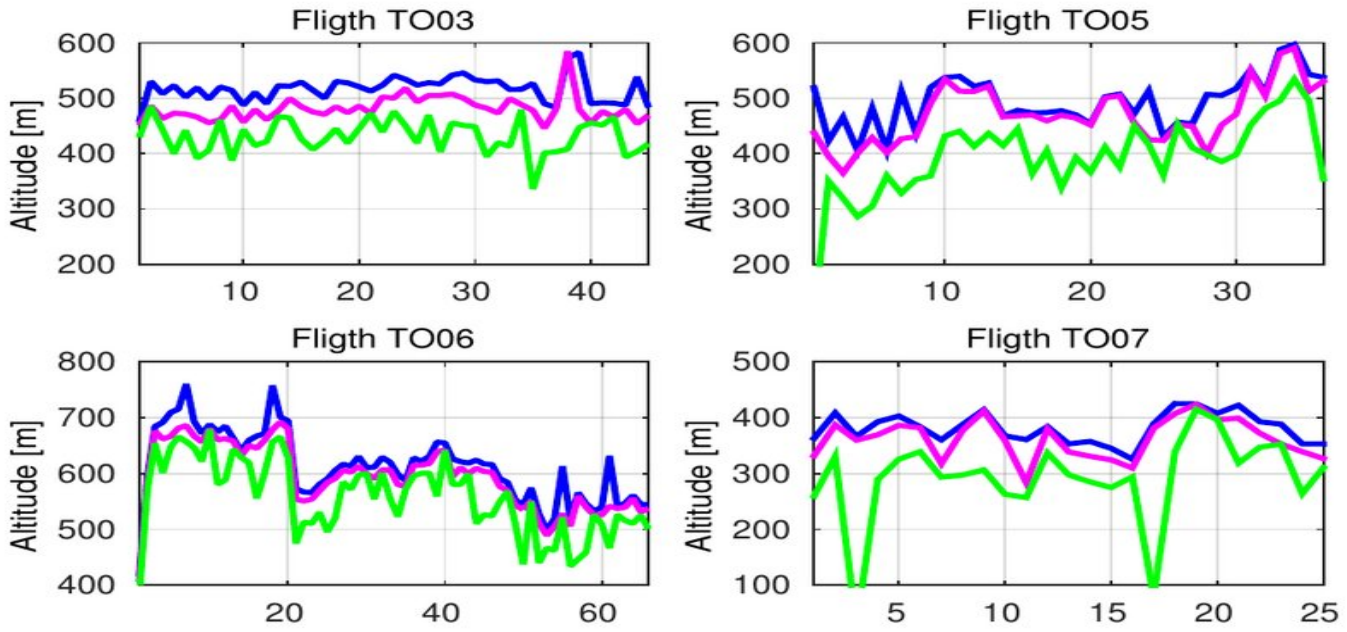

Example: typical layer thickness

TISL:
15 – 35 m

CTMSL:
25 – 75 m

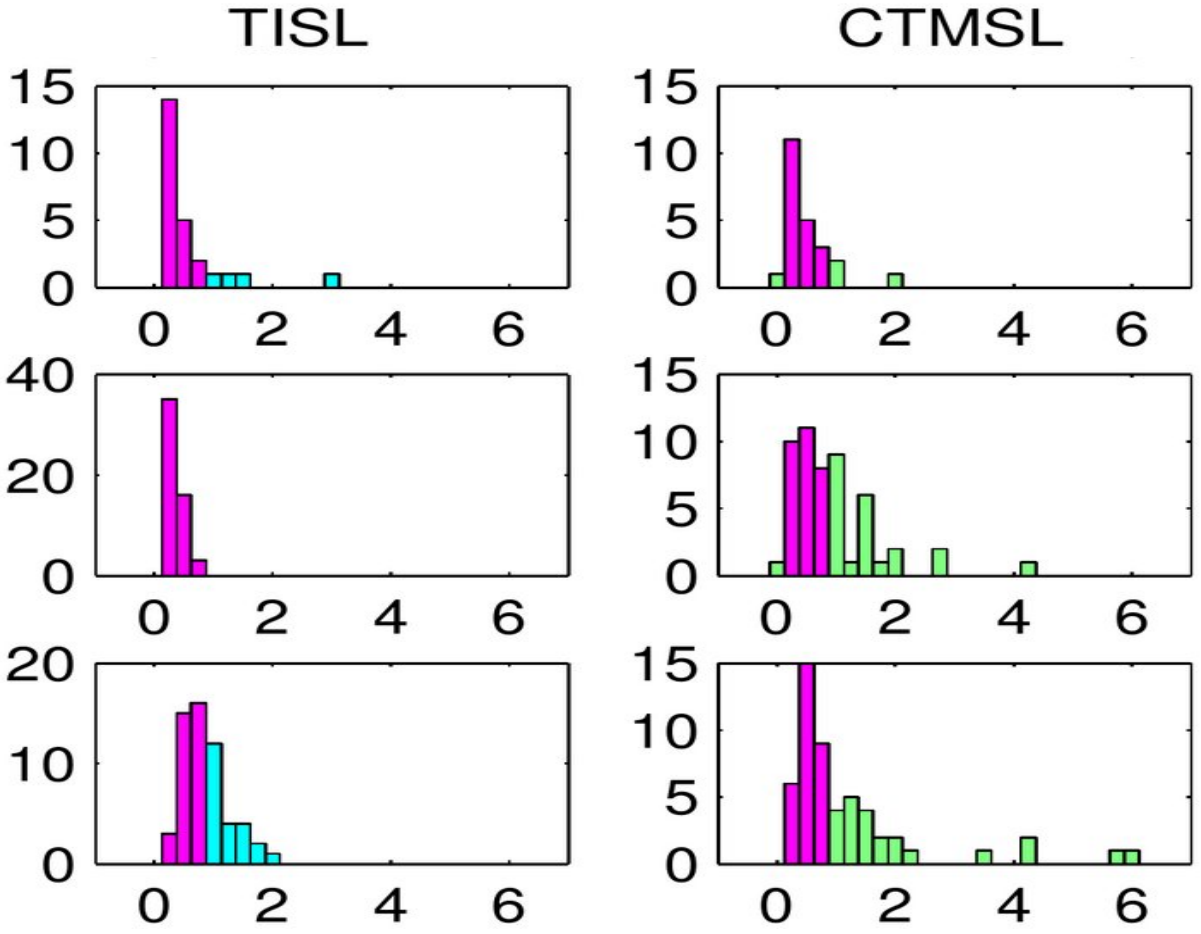

Gradient (bulk) Richardson number:

$$R_i = \frac{\frac{g}{\theta}\left(\frac{\Delta\theta}{\Delta z}\right)}{\left(\frac{\Delta u}{\Delta z}\right)^2 + \left(\frac{\Delta v}{\Delta z}\right)^2}$$

is critical in TISL and CTMSL.

These layers are marginally turbulent.

$$\Delta Z = R_{iC}\left(\frac{\theta}{g}\right)\left(\frac{\Delta u^2 + \Delta v^2}{\Delta\theta}\right)$$

Corrsin and Ozmidov scales:

$$L_C = \sqrt{\varepsilon / S^3}$$

$$L_O = \sqrt{\varepsilon / N^3}$$

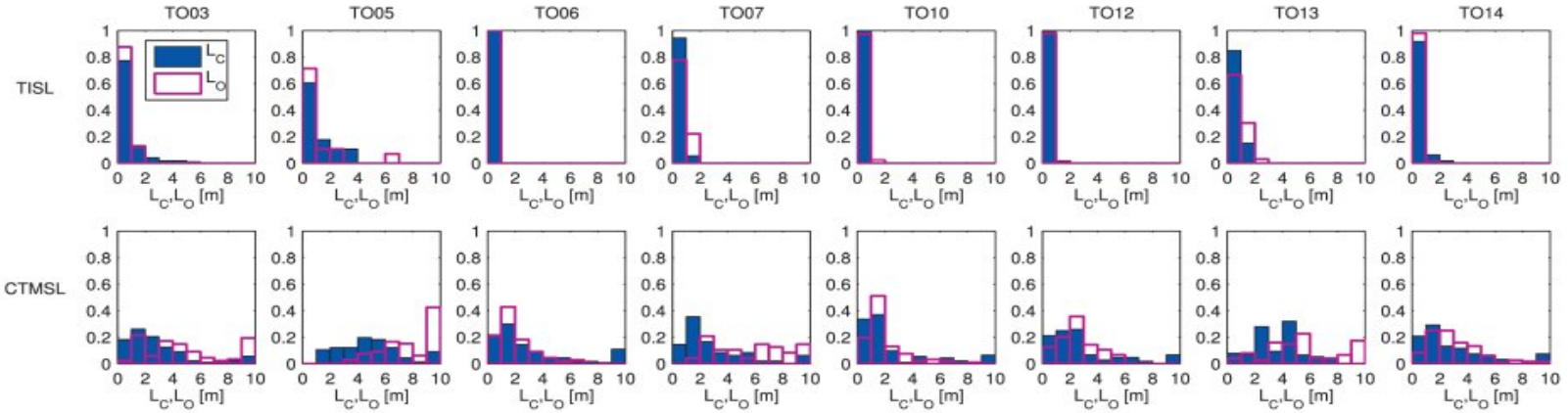

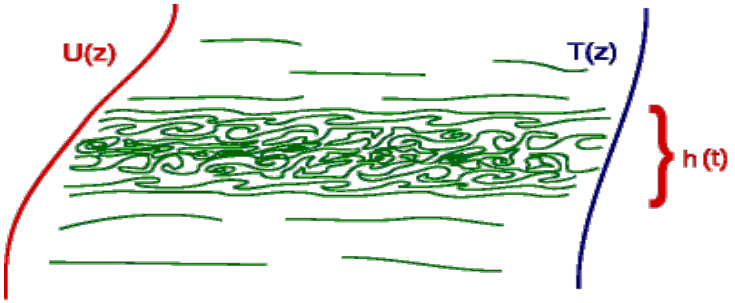

~30 cm in TISL and ~3 m in CTMSL

Eddies larger then these scales flattened and elongated in horizontal !

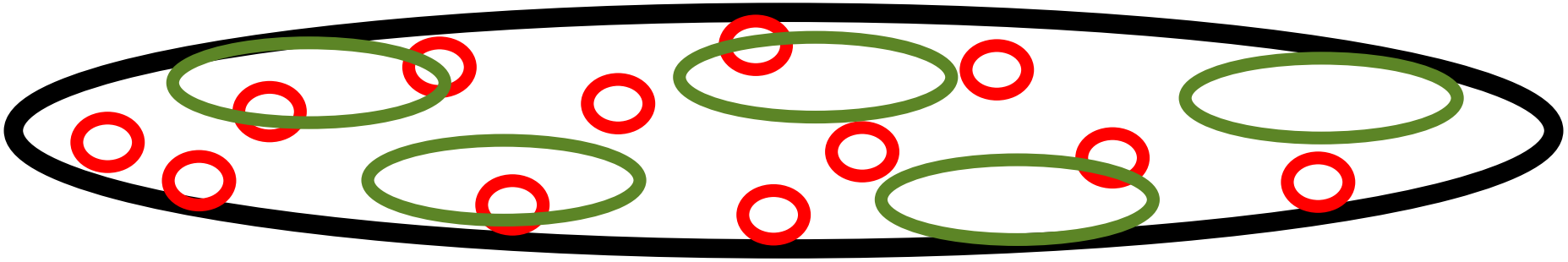

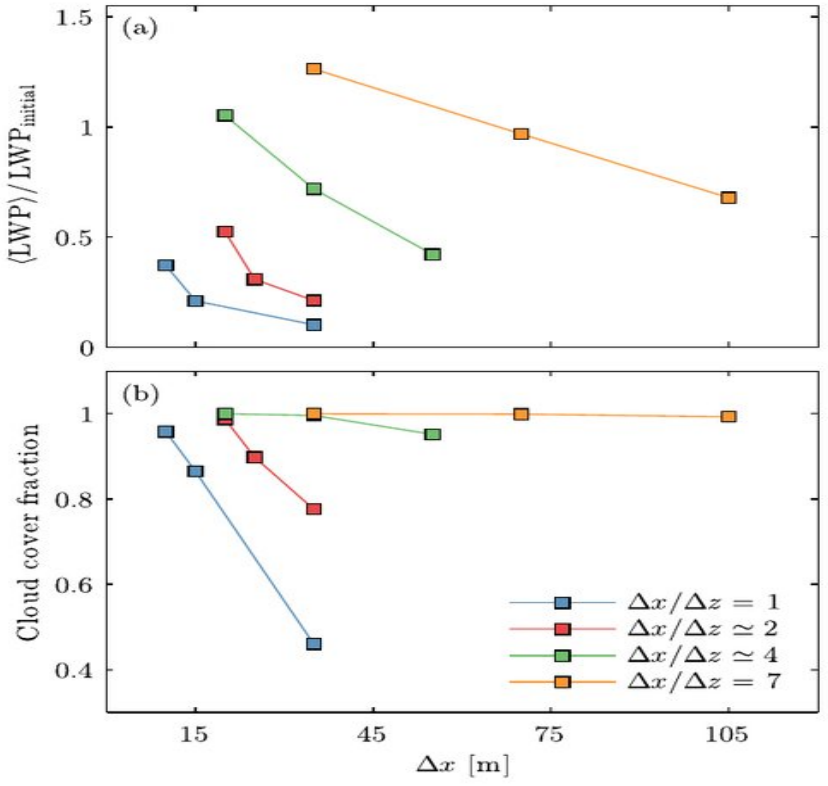

Domain-averaged LWP relative to the initial value
and cloud cover fraction as functions of computational grid anisotropy.

In LES of Sc clouds anisotropic grids do better than isotropic!

Pedersen, J. G. et al., 2016: Resolution and domain-size sensitivity in implicit large-eddy simulation of thestratocumulus-topped boundary layer, *J. Adv. Model. Earth Syst.*, 8, 885–903.

Anisotropic grid:

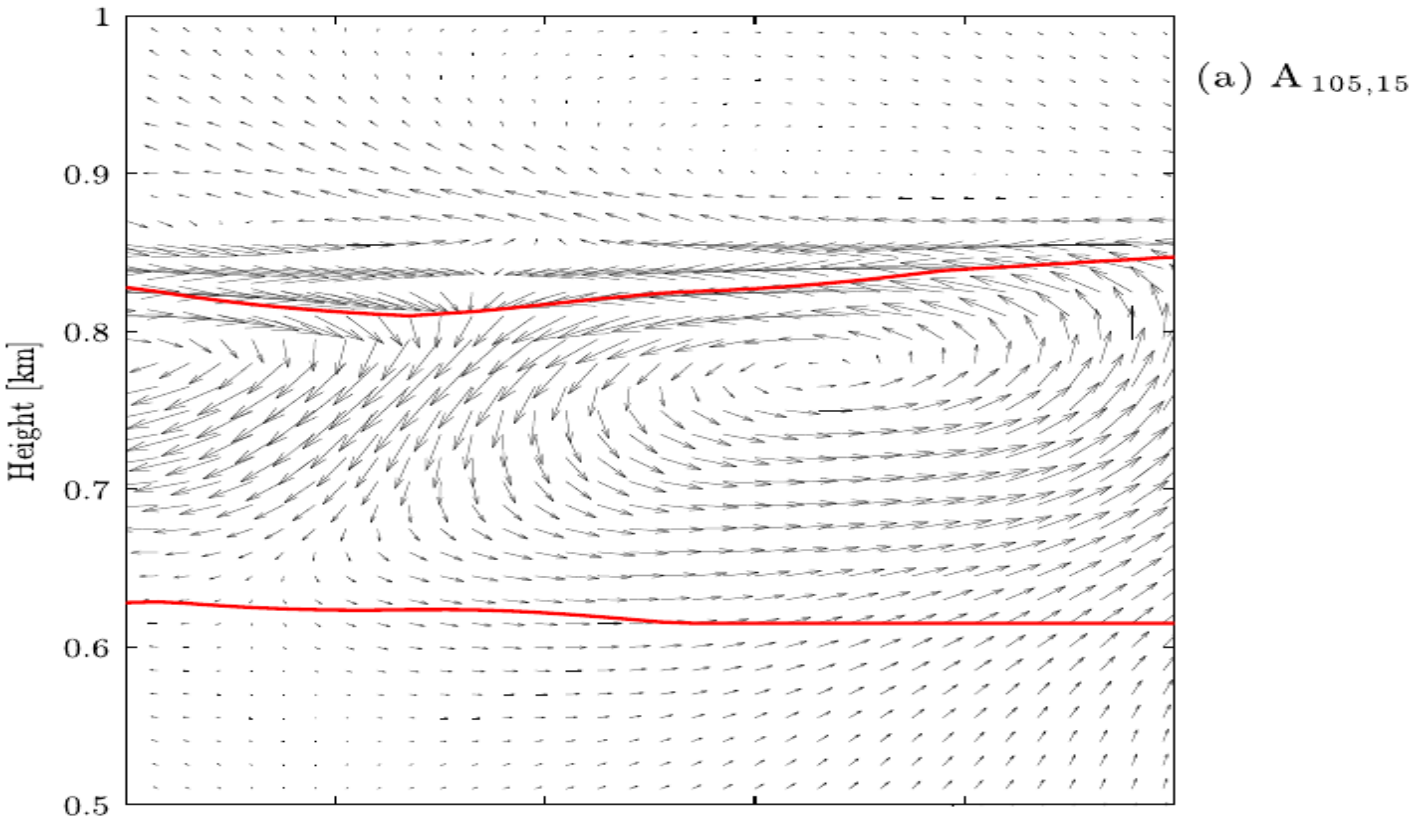

Isotropic grid:

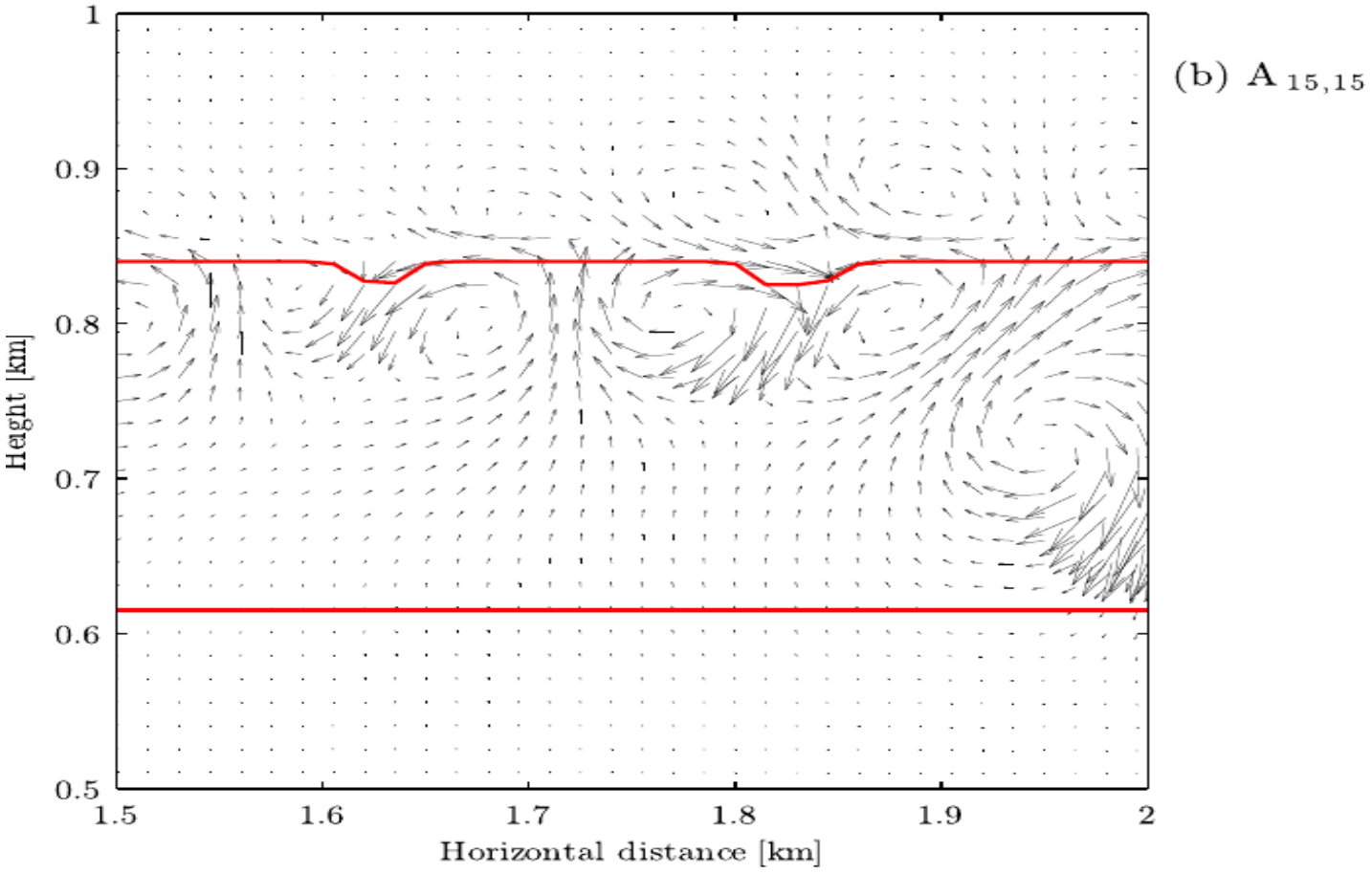

(b) $A_{15,15}$

Lessons from POST:

- there is a lot of anisotropic turbulence due to shear and static stability close to the top of STBL;

- anisotropic turbulence effects in anisotropic transport, which explains problems with modeling and interpretation of entrainment into Sc;

- anisotropy can be characterized, even using standard approaches (velocity variances, spectra);

- anisotropy can be scale-dependent.

ACORES: sampling strategy

Closely collocated (~30 cm) high-resolution instruments

Moderate TAS (~20 m/s)

Siebert, H., et al, 2021: Observations of Aerosol, Cloud, Turbulence, and Radiation Properties at the Top of the Marine Boundary Layer over the Eastern North Atlantic Ocean: The ACORES Campaign, *Bull. Amer. Meteoro.l Soc.*, 102, E123-E147.

Siebert et al. 2021

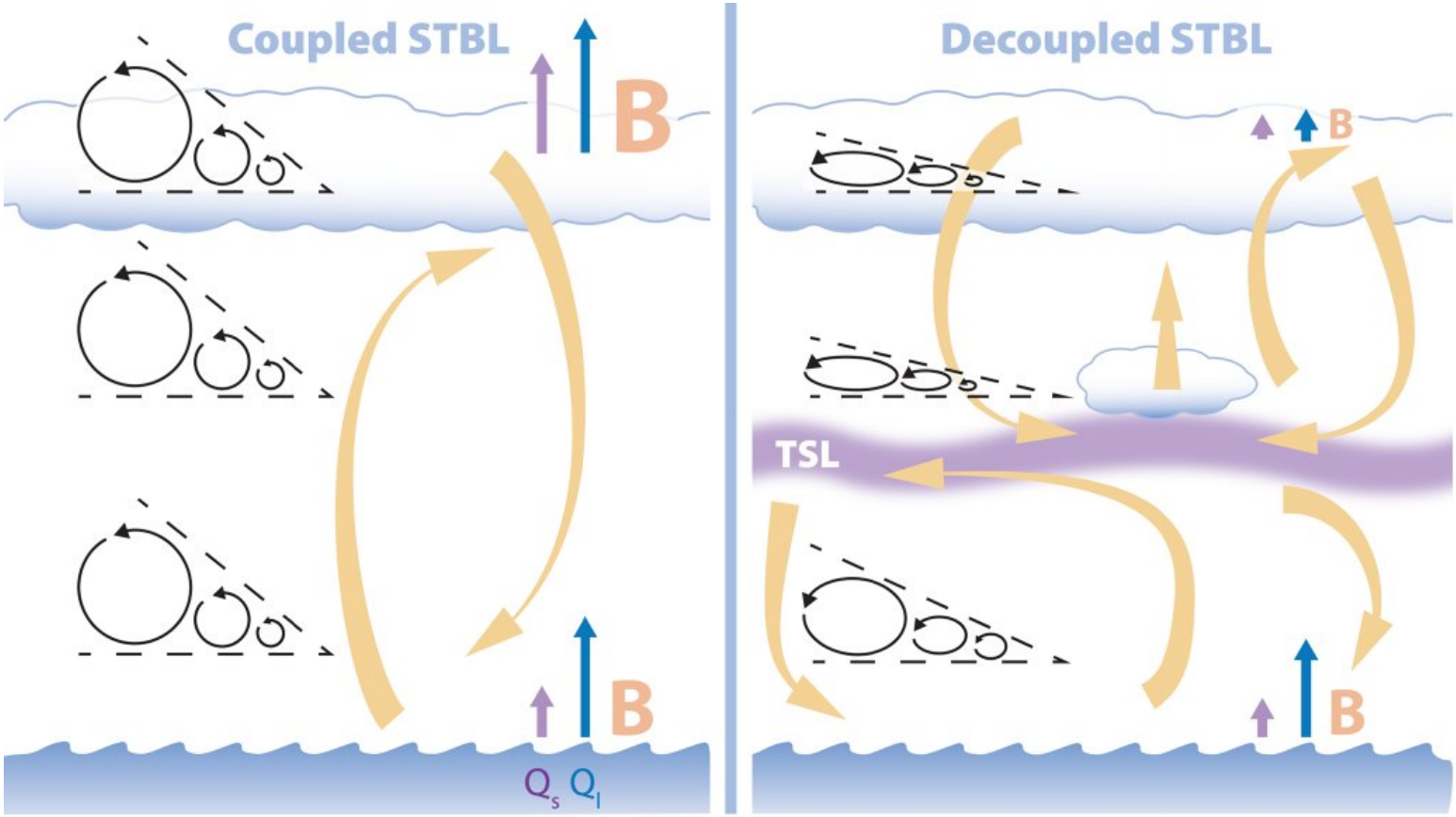

Schematic of main processes in the coupled (left) and decoupled (right) STBLs: primary circulation (yellow arrows), turbulence eddy cascade (circular arrows confined in an angle with extent proportional to inertial range scaling exponent p), TKE buoyancy production (B letter of size proportional to strength), sensible and latent heat fluxes (purple and blue arrows, respectively, of length proportional to strength) at the surface and in the cloud-top region.

Nowak, J. L.et al., 2021: Coupled and decoupled stratocumulus-topped boundary layers: turbulence properties, *Atmos. Chem. Phys.*, 21, 10965–10991.

TKE and variances

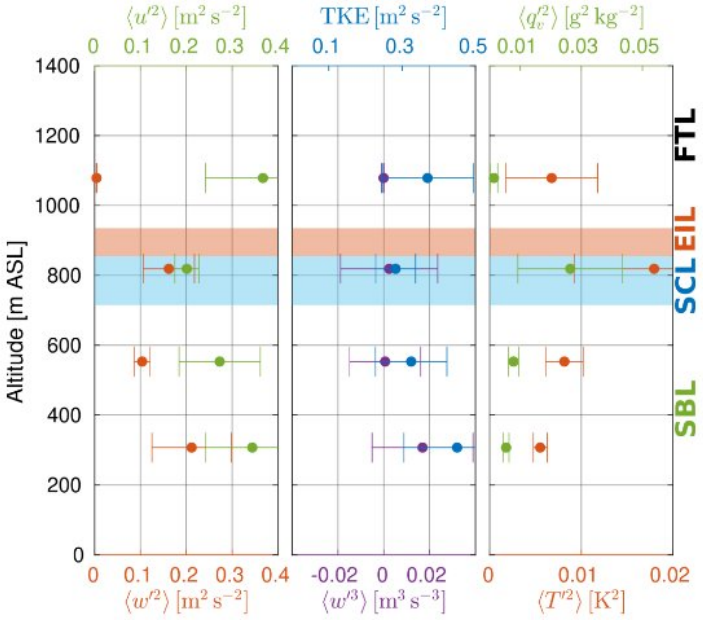

Coupled STBL

$$TKE = \langle u'^2 \rangle + \frac{1}{2}\langle w'^2 \rangle$$

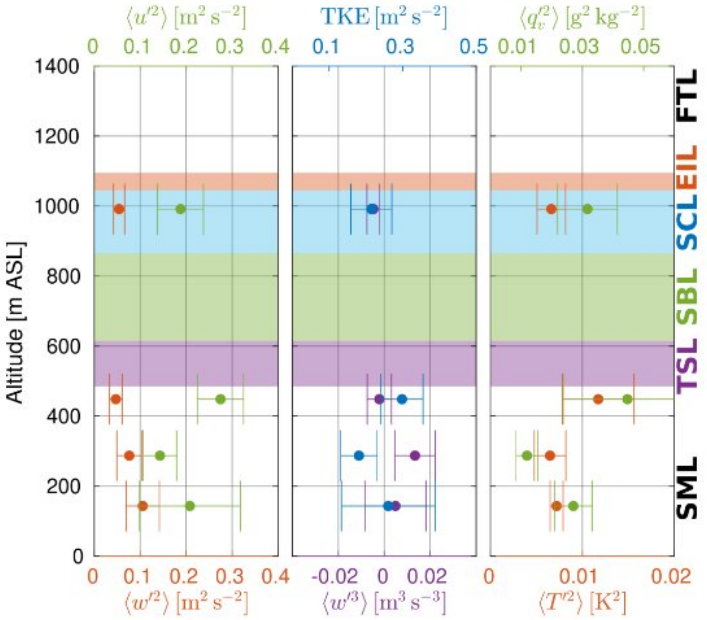

Decoupled STBL

TKE dissipation rate and inertial range scaling

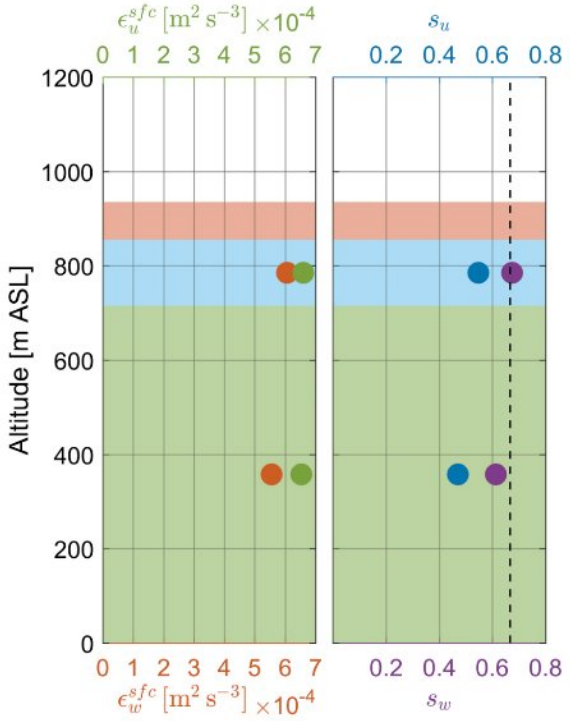

Coupled boundary layer

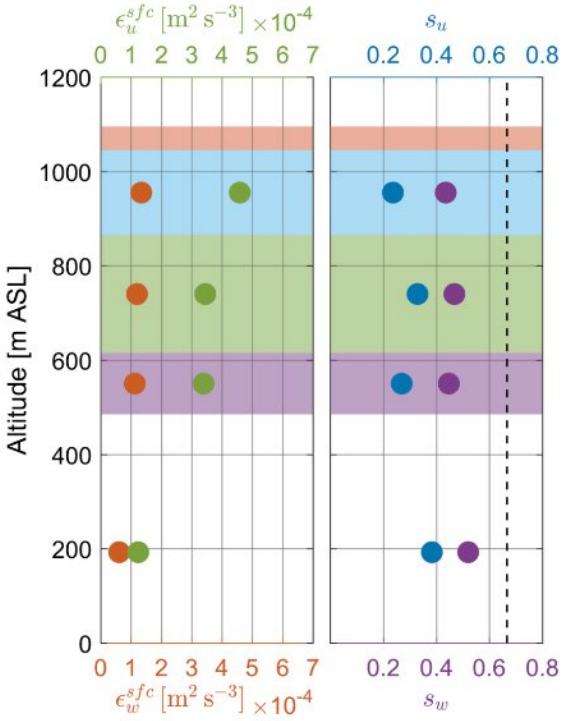

Decoupled boundary layer

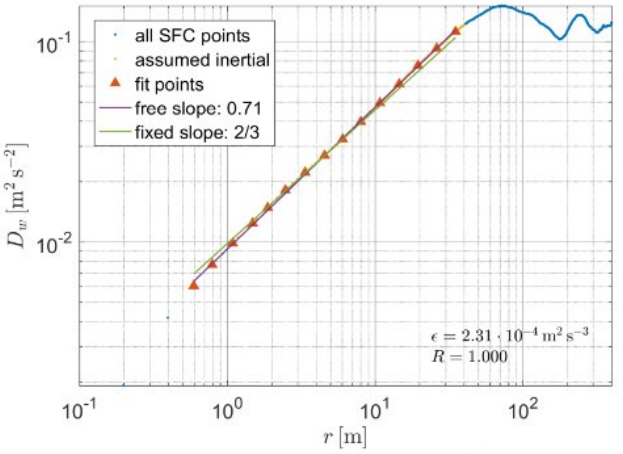

$$D(r) = C_{sfc}(\epsilon r)^{\frac{2}{3}}$$

$$D(r) = C_{sfc}^{*} r^{s}$$

$$D_u \rightarrow \epsilon_u^{sfc}, s_u \quad D_w \rightarrow \epsilon_w^{sfc}, s_w$$

Length scales

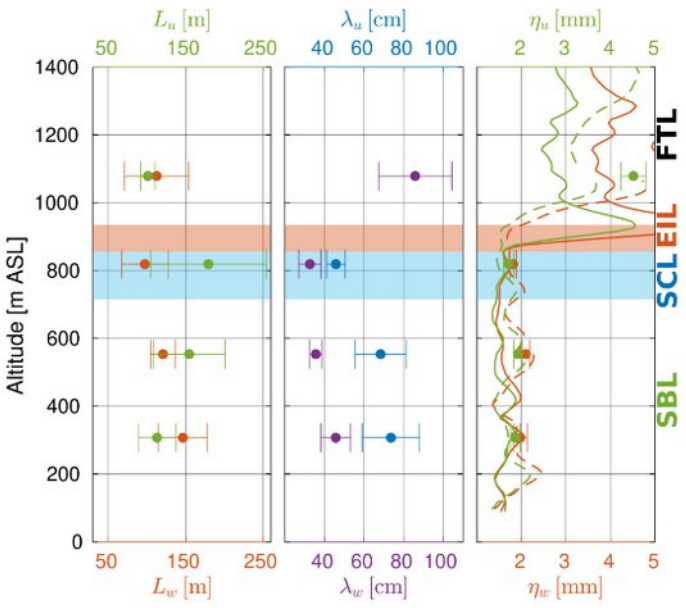

Coupled STBL

$$\rho_u(r) = \frac{\langle u'(x+r)u'(x)\rangle}{\langle u'^2\rangle}$$

$$L_u = \int_0^\infty \rho(r)dr$$

$$\lambda_u = \sqrt{\frac{30\nu\langle u'^2\rangle}{\epsilon_u}} \quad \lambda_w = \sqrt{\frac{15\nu\langle w'^2\rangle}{\epsilon_w}}$$

$$\eta_u = \left(\frac{\nu^3}{\epsilon_u}\right)^{\frac{1}{4}}$$

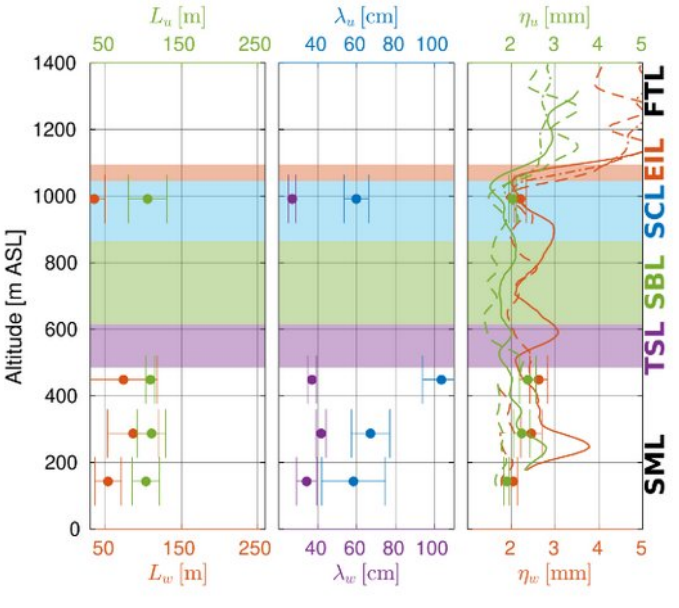

Decoupled STBL

Anisotropy

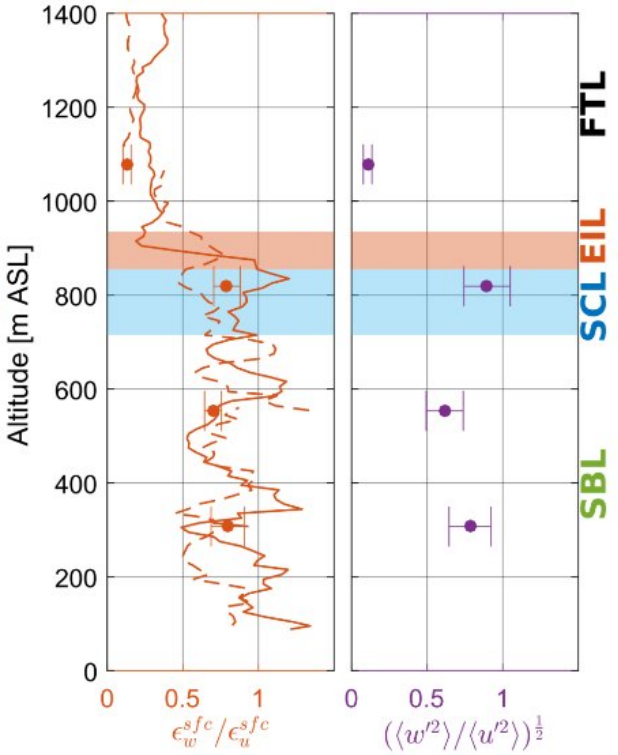

Coupled STBL

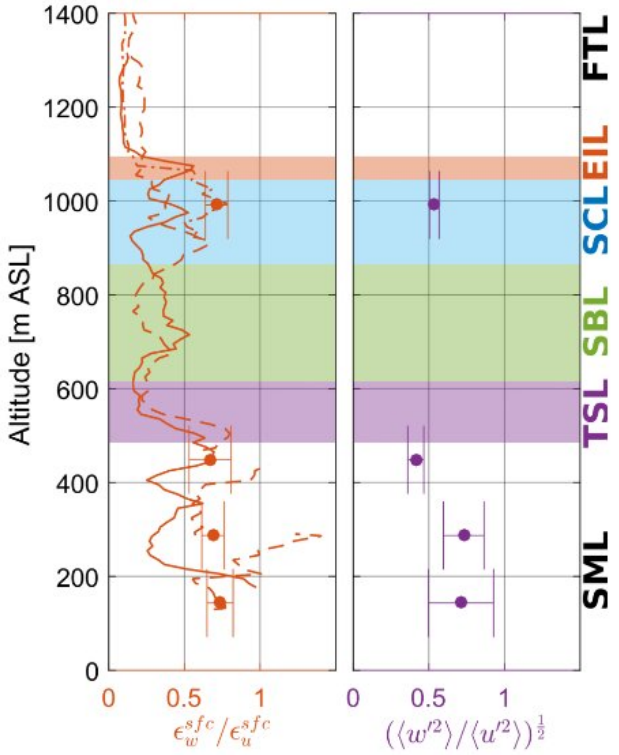

Decoupled STBL

Lessons from ACORES:

- there is a lot of anisotropy in turbulence not only close to the cloud top, but across the whole BL depth and across scales;

- integral scales of turbulence are ~100m, i.e. turbulence is not responsible for transport across BL layers, convective circulations do the job.

- there are differences in turbulence across and within the layers.

Nonstationarity:

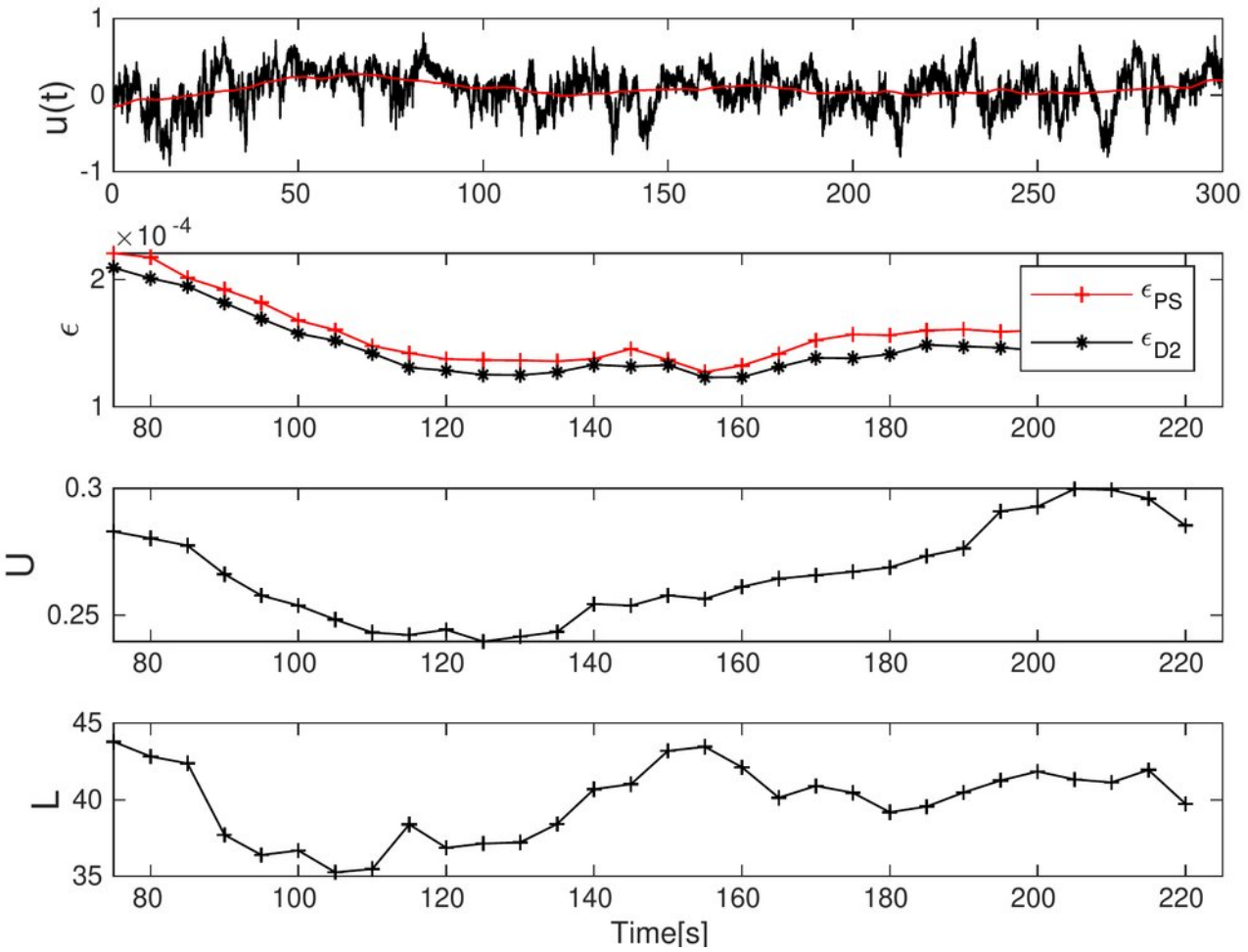

a) Wind velocity measured along the flight track,

b) dissipation rates estimated from one-dimensional spectra and structure functions under assumption of local isotropy,

c) velocity scale $\mathcal{U}$ ($\mathcal{U}^2$ = 2/3E)

d) integral length scale $\mathcal{L}$

Idealized spectrum of homogeneous and stationary turbulence

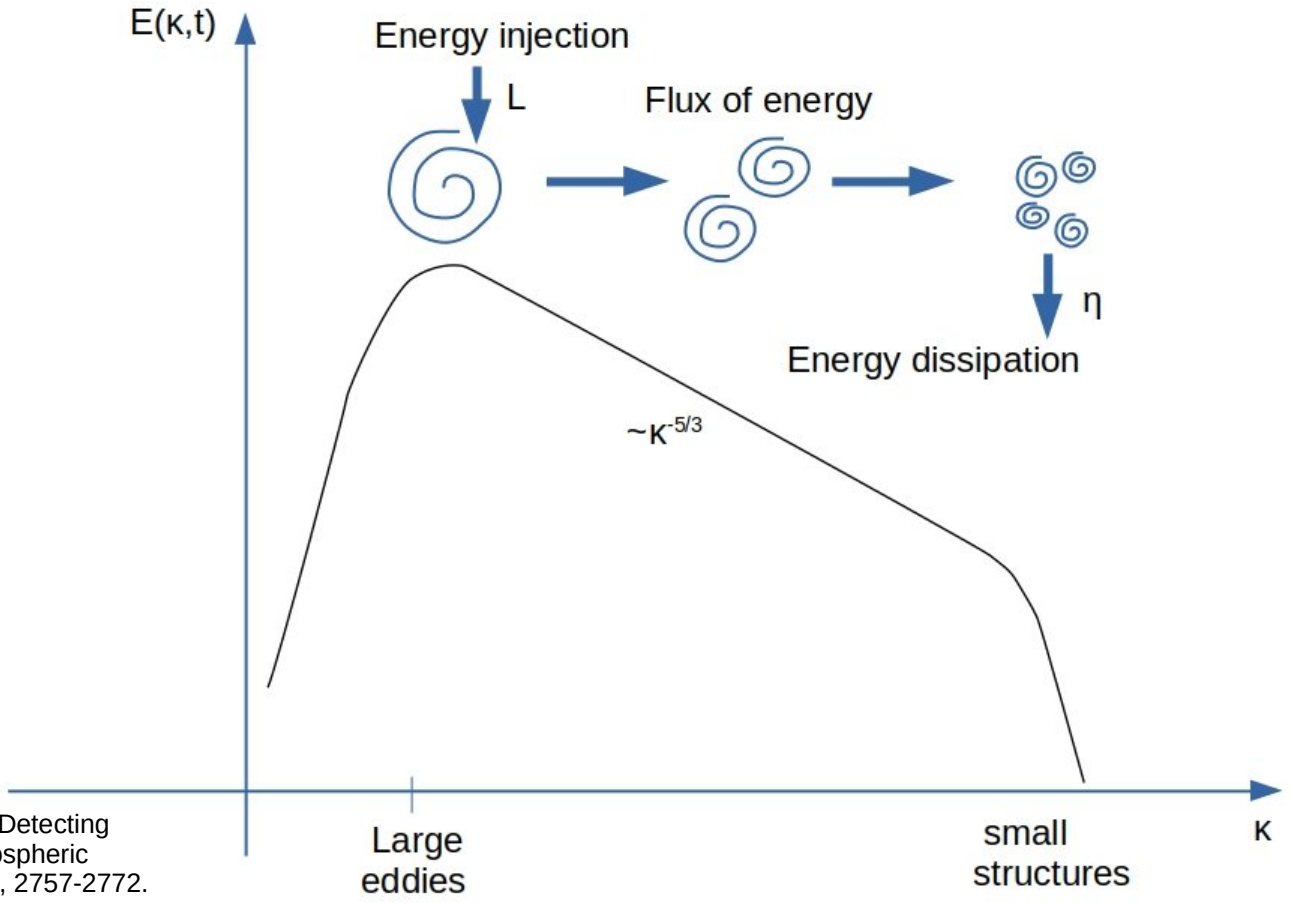

Wacławczyk, M., et al., 2022: Detecting Nonequilibrium States in Atmospheric Turbulence, *J. Atmos. Sci.*, 79, 2757-2772.

Developing turbulence

Decaying turbulenve

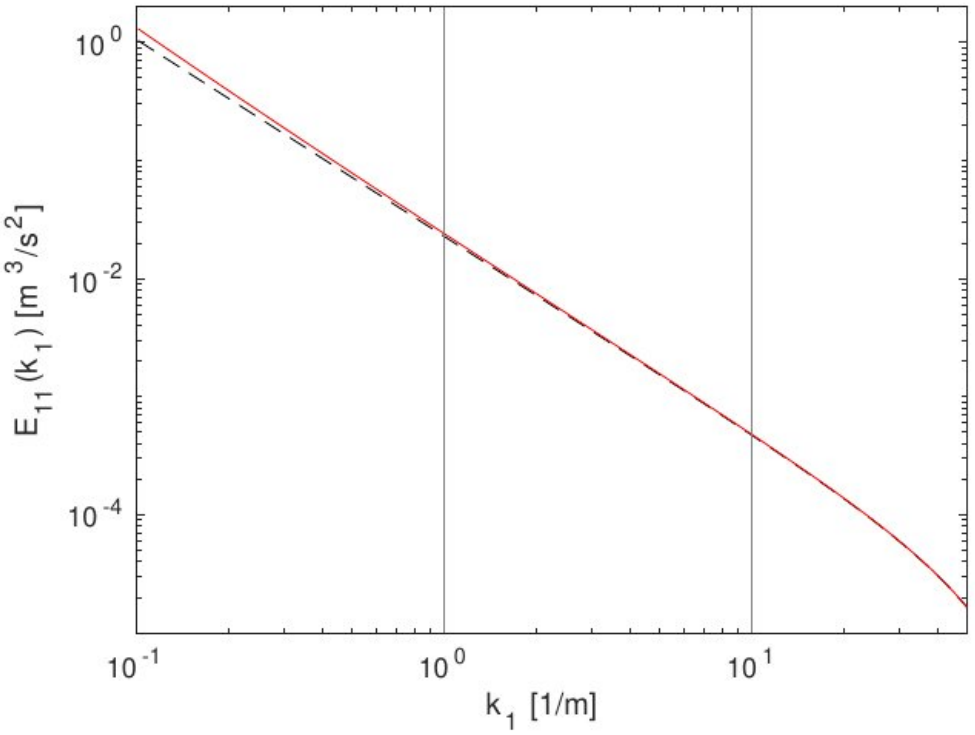

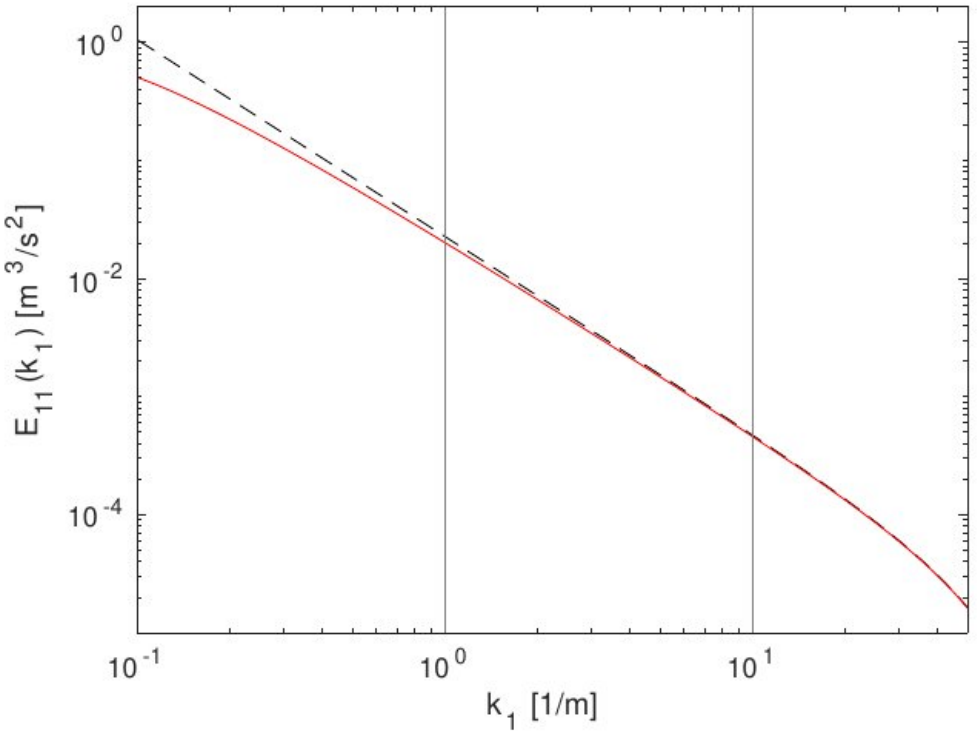

Wacławczyk, M., et al., 2022: Detecting Nonequilibrium States in Atmospheric Turbulence, *J. Atmos. Sci.*, 79, 2757-2772.

Non-equilibrium one-dimensional spectra.

Equilibrium Taylor's law:

$$C_\epsilon = \epsilon \frac{\mathcal{L}}{\mathcal{U}^3} = const$$

Research works of Seoud & Vassilicos [Physics of Fluids, **19**, 2007], Valente & Vassilicos [Physics of Fluids, **27**, 2015] revealed an "unusual", although universal dissipation scaling in decaying grid turbulence.

Non-equilibrium law

$$C_\epsilon = \epsilon \frac{\mathcal{L}}{\mathcal{U}^3} \sim \frac{Re_0^m}{Re_\lambda^n},$$

where $Re_0 = U_\infty L_b/\nu$, $m, n \approx 1$

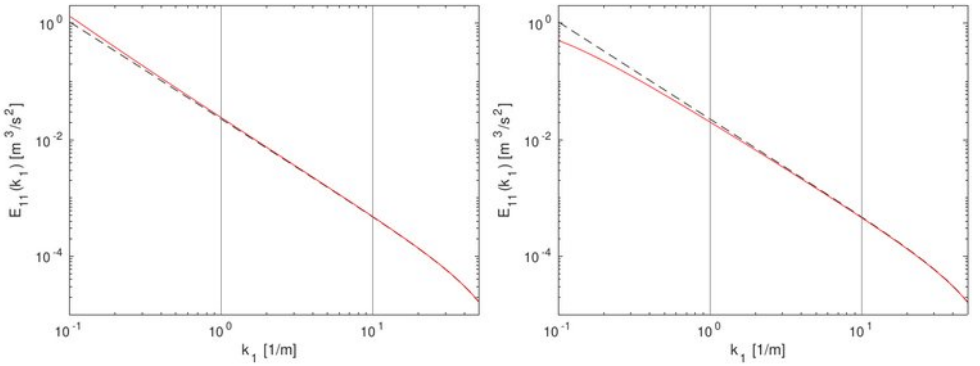

Non-equilibrium turbulence
(Bos & Rubinstein [Phys. Rev. Fluids, **2**, 2018]):

$$E(\kappa, t) = E_0(\kappa, t) + \widetilde{E}(\kappa, t) + \cdots ,$$

where

$$E_0(\kappa, t) = C_K \epsilon^{2/3} \kappa^{-5/3},$$

and

$$\widetilde{E}(\kappa, t) = C_K^2 \frac{2}{3} \frac{\dot{\epsilon}}{\epsilon^{2/3}} \kappa^{-7/3},$$

where

$$\dot{\epsilon} = \frac{\mathrm{d}\epsilon}{\mathrm{d}t}$$

Equilibrium:

$$C_\epsilon = const, \quad \frac{\mathcal{L}}{\lambda} = \frac{C_\epsilon}{15} Re_\lambda,$$

Non-equilibrium (Bos & Rubinstein [Phys. Rev. Fluids, **2**, 2018]):

$$C_\epsilon \approx C_{\epsilon 0} Re_{\lambda 0}^{15/14} \left(\frac{1}{Re_\lambda}\right)^{15/14}, \quad \frac{\mathcal{L}}{\lambda} \approx \frac{C_{\epsilon 0} Re_{\lambda 0}^{15/14}}{15} \left(\frac{1}{Re_\lambda}\right)^{1/14},$$

- $C_\epsilon > C_{\epsilon 0}$ — weak turbulence production, as $\dot{\epsilon} < 0$
- $C_\epsilon < C_{\epsilon 0}$ — strong turbulence production, as $\dot{\epsilon} > 0$
- $C_\epsilon = C_{\epsilon 0}$ — stationary states, $\dot{\epsilon} = 0$

$$C_\epsilon = const, \qquad \text{vs.} \qquad C_\epsilon \approx C_{\epsilon 0} Re_{\lambda 0}^{15/14} \left(\frac{1}{Re_\lambda} \right)^{15/14},$$

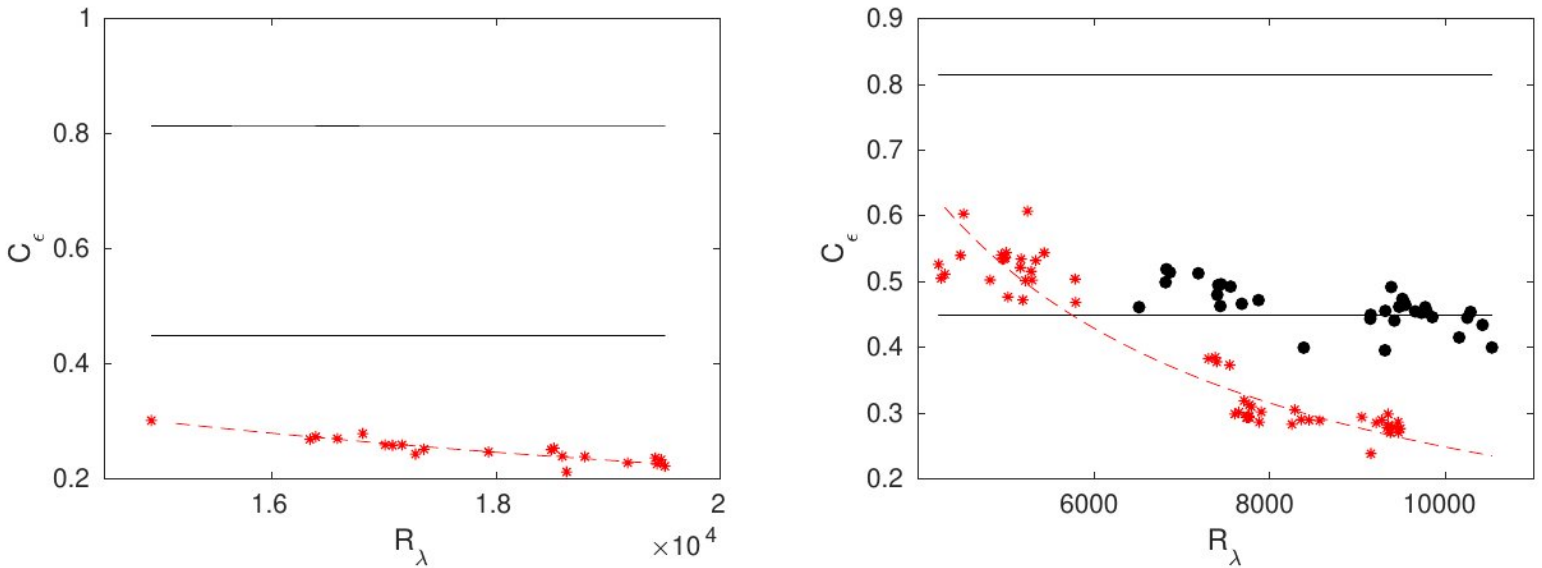

C_ε as a function of Re_λ .
Solid black lines - equilibrium scalings, $C_{\varepsilon 0} = 0.45$ and $C_{\varepsilon 1} = 1.81 C_{\varepsilon 0}$, dashed red line - non-equilibrium scaling calculated statistics: symbols.
a) coupled STBL, LEG5, b) decoupled STBL, LEG2.

$$\frac{\mathcal{L}}{\lambda} = \frac{C_\epsilon}{15} Re_\lambda, \qquad \text{vs.} \qquad \frac{\mathcal{L}}{\lambda} \approx \frac{C_{\epsilon 0} Re_{\lambda 0}^{15/14}}{15} \left(\frac{1}{Re_\lambda}\right)^{1/14},$$

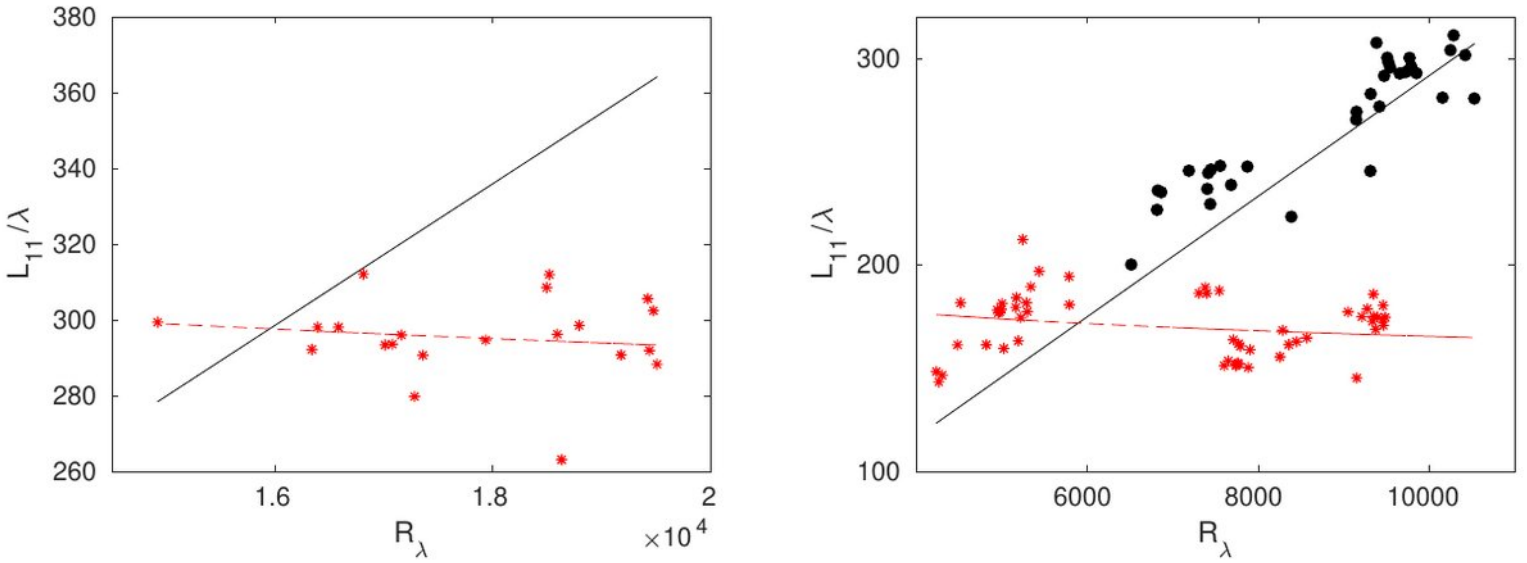

$\mathcal{L}/\lambda$ as a function of Re_λ . Solid black line - equilibrium scaling, dashed red line - non-equilibrium scaling, calculated statistics: symbols.
a) coupled STBL, LEG5, b) decoupled STBL, LEG2.

More lessons from ACORES:

$$C_\epsilon = \epsilon \frac{\mathcal{L}}{\mathcal{U}^3}$$

- it is possible to classify turbulent stationarity/nonstationarity with the use of non-dimensional indicators C_ε and $\mathcal{L}/\lambda$ on segments long enough to estimate ε, yet short enough to not average on regions of different turbulence properties;

- coupled STBL is characterized by lower values of C_ε (stronger turbulence production) than decoupled STBL,

- regions of non-equilibrium turbulence prevailed in decoupled STBL, which indicates rapidly changing conditions.

EUREC-4A/ATOMIC

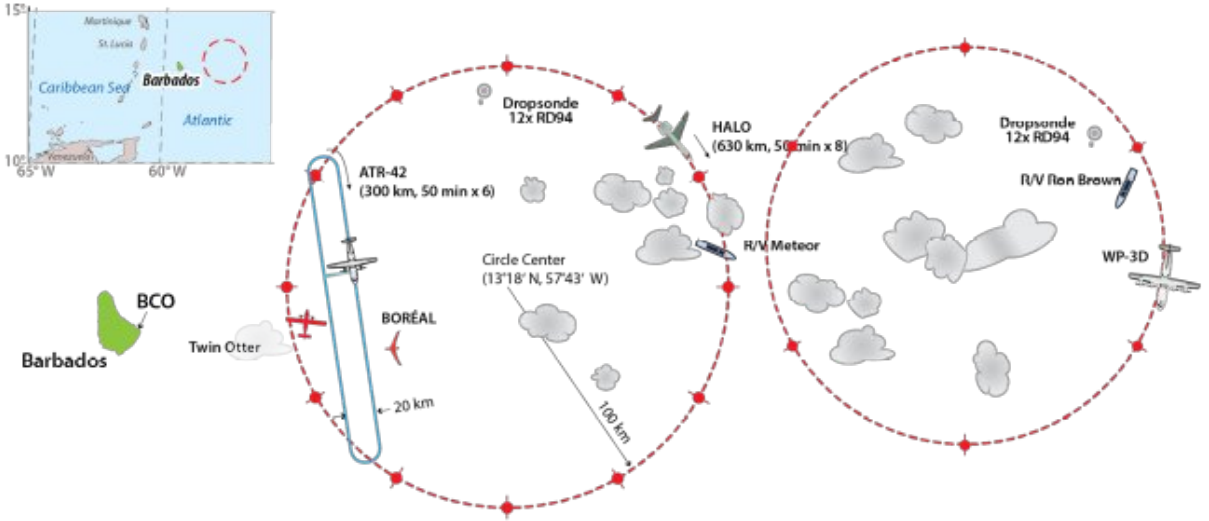

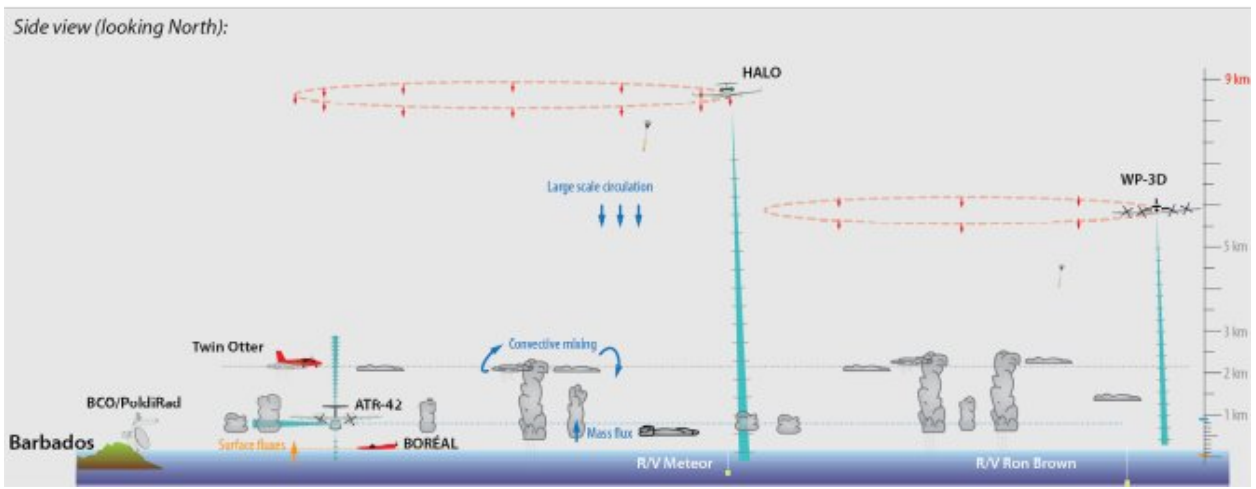

Stevens, B., et al., 2021: EUREC4A, *Earth Syst. Sci. Data*, 13, 4067–4119.

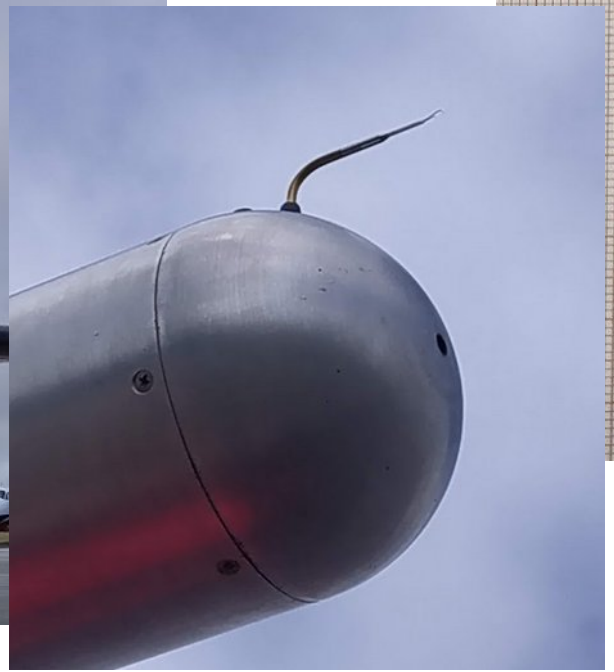

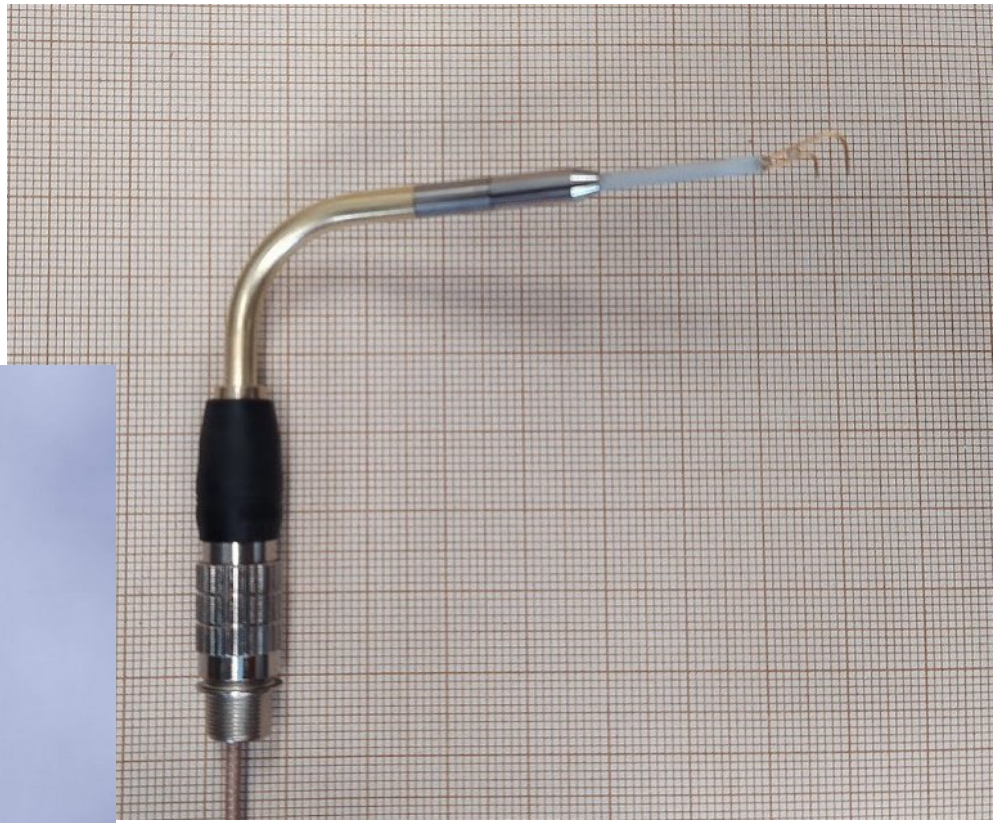

A special version of the UFT mounted on the turbulence probe of BAS Twin Otter

BAS TO – a selected segment of flight 336

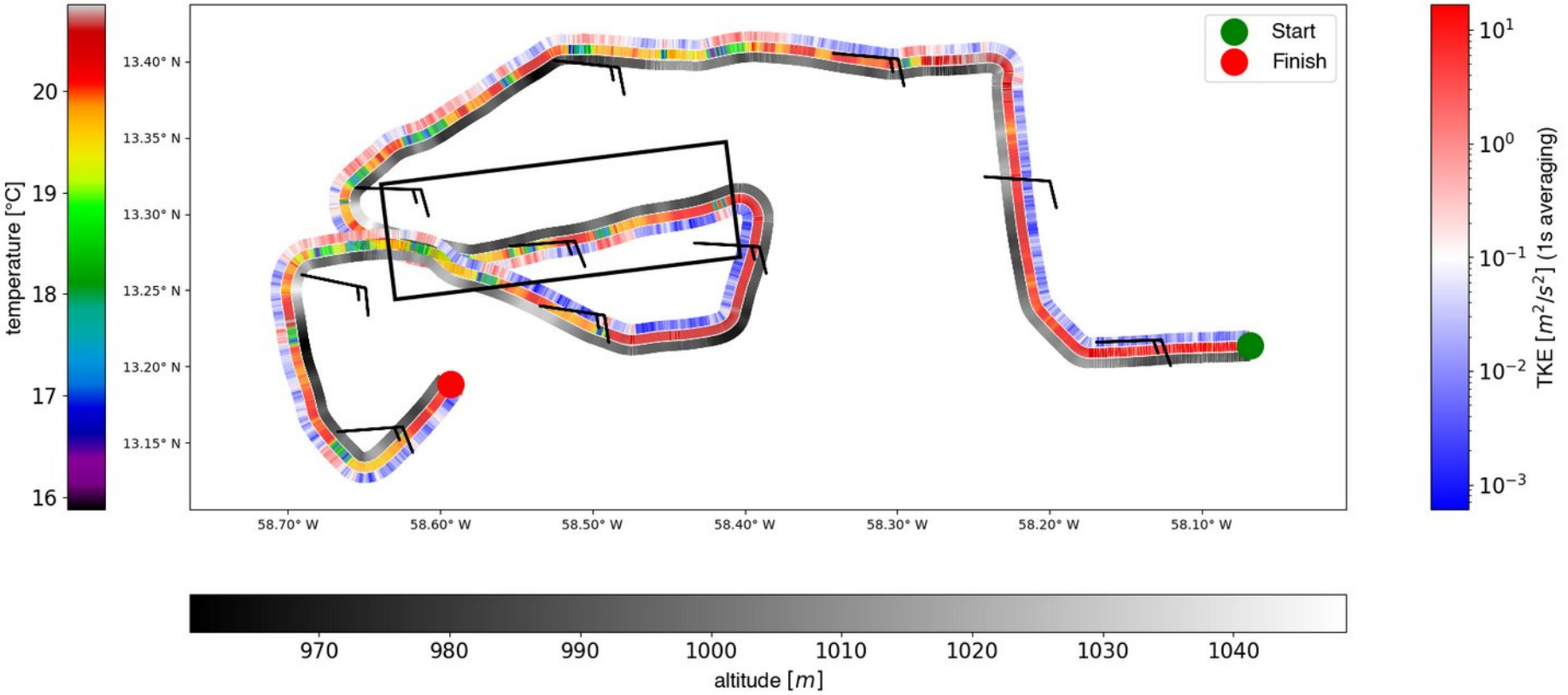

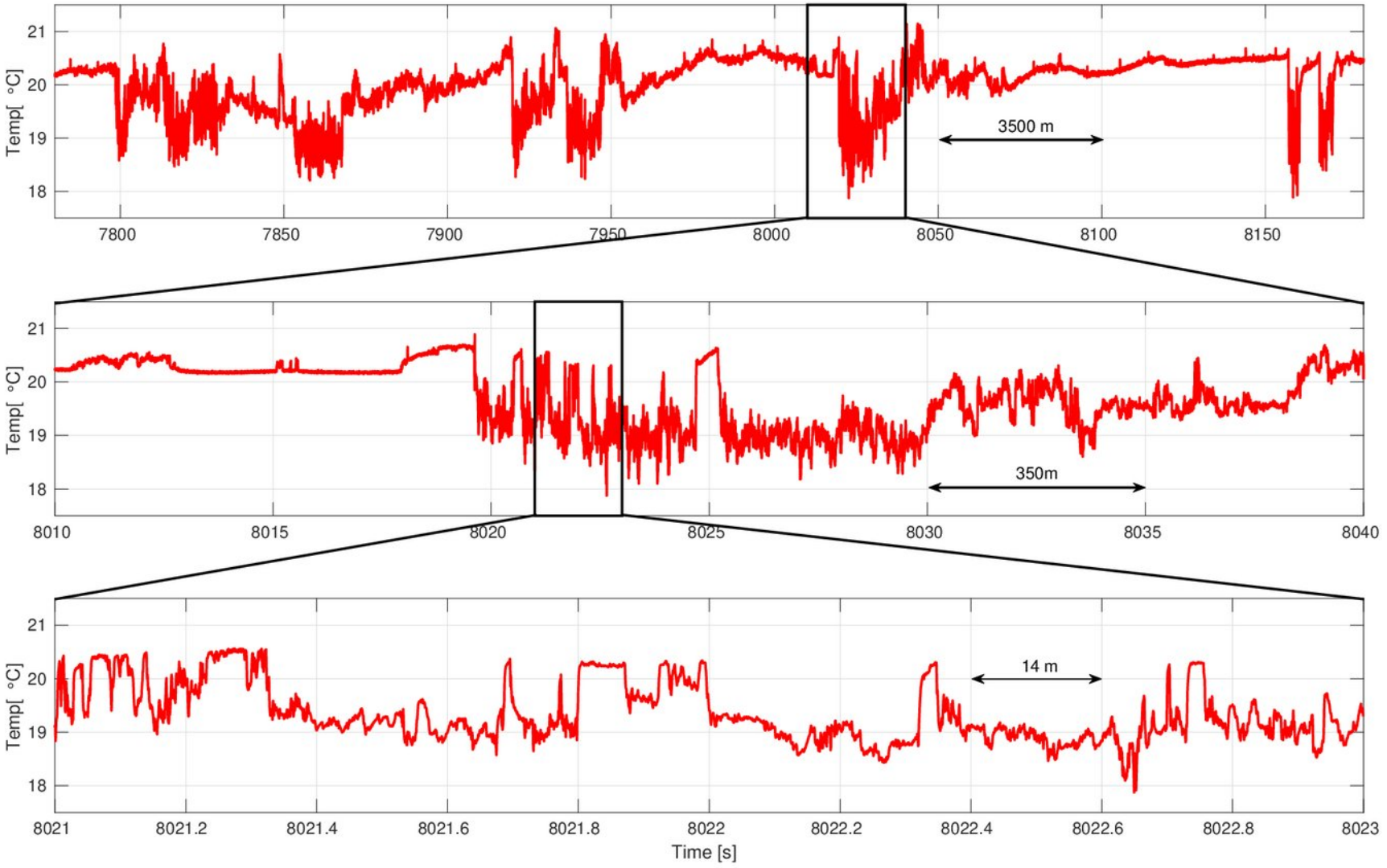

UFT2 temperature

Application of Recurrence Quantification Analysis to objectively account for nonhomogeneity of turbulence and prepare segments of data for turbulence analysis

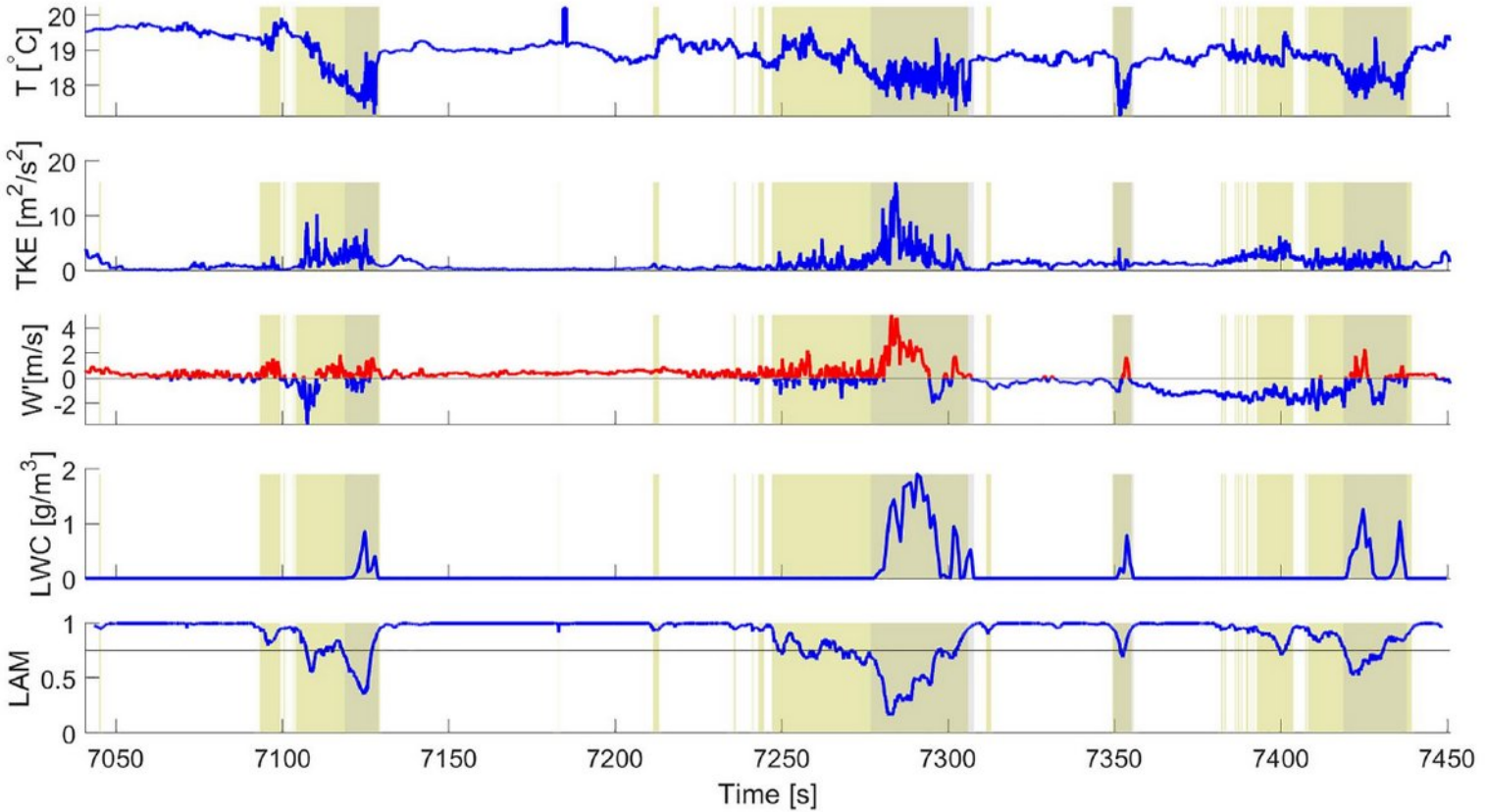

Król, S., Blyth, A., Böing, S., Denby, L., Lachlan-Cope, T., & Malinowski, S. P. (2024). Can recurrence quantification analysis be useful in the interpretation of airborne turbulence measurements? Geophysical Research Letters, 51, e2023GL105753. https://doi.org/10.1029/2023GL105753

Table 1

Values of the Mean TKE, and Standard Deviations of the Temperature and the Vertical Wind Velocity Variable Component for Three Different Masks: $LAM^{>}$*–*LAM *Above 0.95 Threshold, LWC–LWC Above Threshold,* $LAM^{<}$*–*LAM *Below 0.95 Threshold, but With LWC Below Threshold*

	$LAM^{>}$	LWC	$LAM^{<}$
μ_k	0.79	2.46	1.51
σ_T	0.32	0.32	0.34
$\sigma_{w'}$	0.58	1.31	0.93

Nowak, J.L., Wacławczyk, M., Vassilicos, J.C., Król, S. & Malinowski, S.P. (2025)

Scale-by-scale budget of turbulence kinetic energy in the convective atmospheric boundary layer: Analysis of structure functions.

Quarterly Journal of the Royal Meteorological Society, 1–18. Available from: https://doi.org/10.1002/qj.4879

Abstract

We investigate the scale-by-scale budget of turbulence kinetic energy in convective atmospheric boundary layers using airborne measurements performed in the shallow trade-wind regime over the ocean by the ATR 42 aircraft during the Elucidating the Role of Cloud–Circulation Coupling in Climate (EUREC4A) measurement campaign. The simple and repeatable flight pattern sampled four altitude levels: near-surface, the middle and top of the subcloud layer, and the cloud base. This approach provides acceptable statistical convergence, including mixed velocity–temperature and third-order velocity structure functions. The scale-by-scale budget obtained from the data is approximately closed up to length-scales of about 200 m at all four levels. At the near-surface and mid-subcloud levels, the buoyancy forcing supplies energy to the largest scales and becomes negligible at smaller scales. As a result, Kolmogorov equilibrium is observed over a wide range of scales, from a few to about 100 m. On the other hand, at the top-subcloud and cloud-base levels, the budget at scales above 10 m is far from Kolmogorov equilibrium, with a significant contribution of buoyancy forcing and turbulent transport. The contribution to the buoyancy forcing related to humidity variations is substantial and strictly positive at all four levels, even at the cloud base, where it balances the negative contribution related to temperature only.

The Kolmogorov 4/5 law form for the ensemble average 3rd order structure function S_3 , which takes into account transverse velocity components, reads:

$$\overline{\delta u^3} + \overline{\delta u\ \delta v^2} + \overline{\delta u\ \delta w^2} = -\frac{4}{5}\epsilon r - \frac{8}{15}\epsilon r = -\frac{4}{3}\epsilon r,$$

$$\delta u = u(\boldsymbol{x} + \boldsymbol{r}) - u(\boldsymbol{x})$$

Dissipation in stationary situation equal energy transfer rate between scales.
Solving under certain assumptions energy budget from the equations of motion allows for analyzing the scale-by scale energy budget and verify it experimentally from airbotne measurements at various heights in the atmospheric boundary layer from close to surface to cloud base:

$$\frac{S_3}{r} = -T - 4\overline{\epsilon} + W,$$

where T is (vertical) transport and W is buoyancy production.

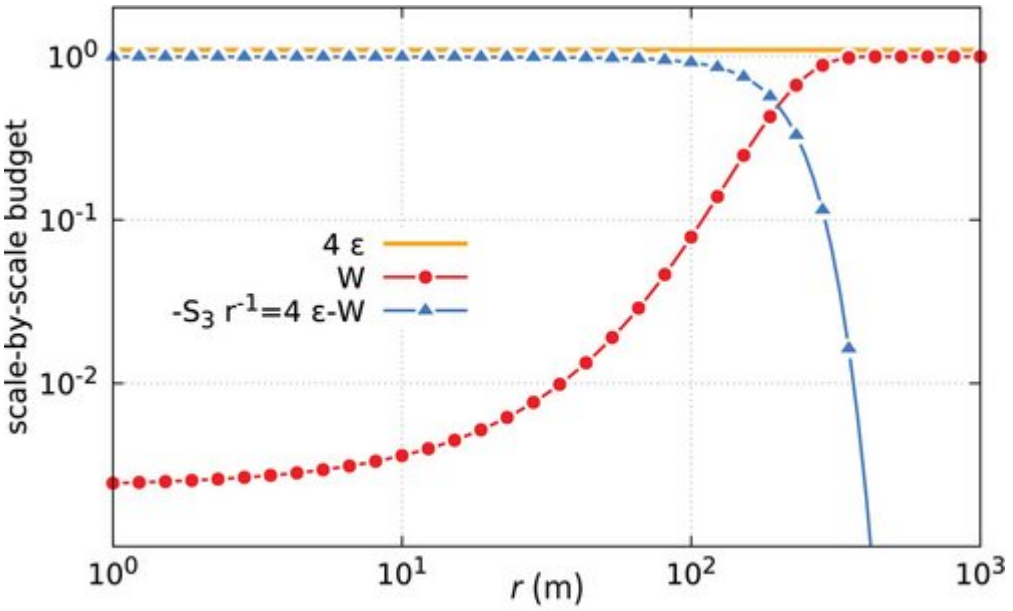

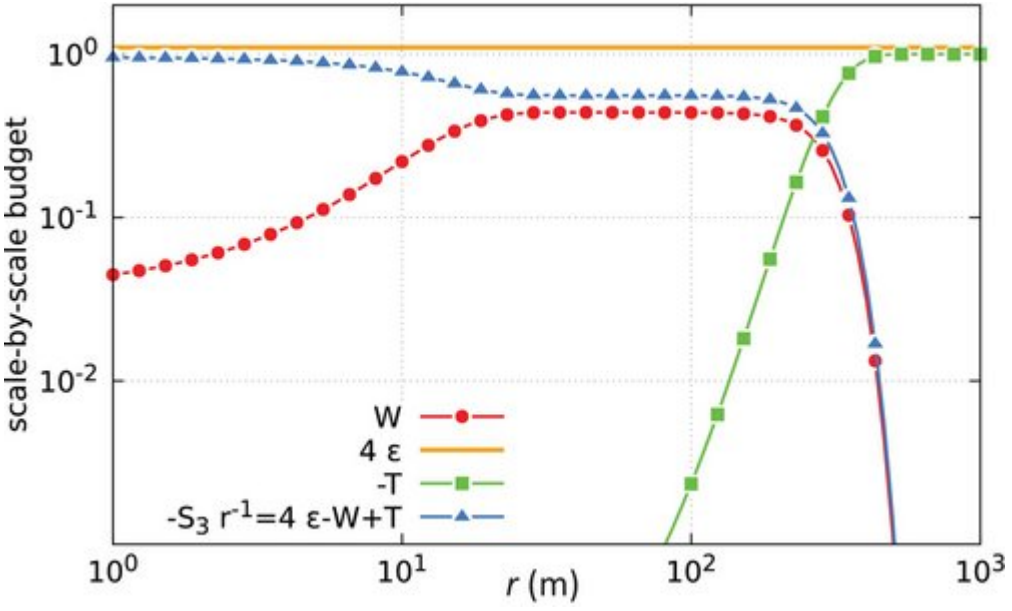

Idealized scale-by-scale energy budget for 1 m in the classical Richardson–Kolmogorov scenario: energy injected at large scales due to buoyancy forcing is transferred to smaller scales and dissipated therein.

Such a picture is observed close to the surface and in the middle of the ABL.

Illustrative approximate scale-by-scale energy budget at the cloud-base and top-subcloud levels:

energy is transported to the system from lower heights (T<0), part of this energy is transferred downscale and dissipated, and another part is used to work against the large-scale stable stratification.

Signature of convection organization !

How to analyze turbulence from in-flight data?

- divide your time series into segments corresponding to similar states of the flow;

- determine integral length scales based on velocity autocorrelations in the regions where you observe similar properties of turbulence;

- for Reynolds averaging select windows of FEW integral length scales, but not too large since turbulence is nonhomogeneous in space;

- quantify velocity variances, TKE, dissipation rate, all relevant scales and other turbulence characteristics like anisotropy, intermittency and stationarity/nonstationarity, organization and transport;

TURBULENCE??? TURBULENCES !!!

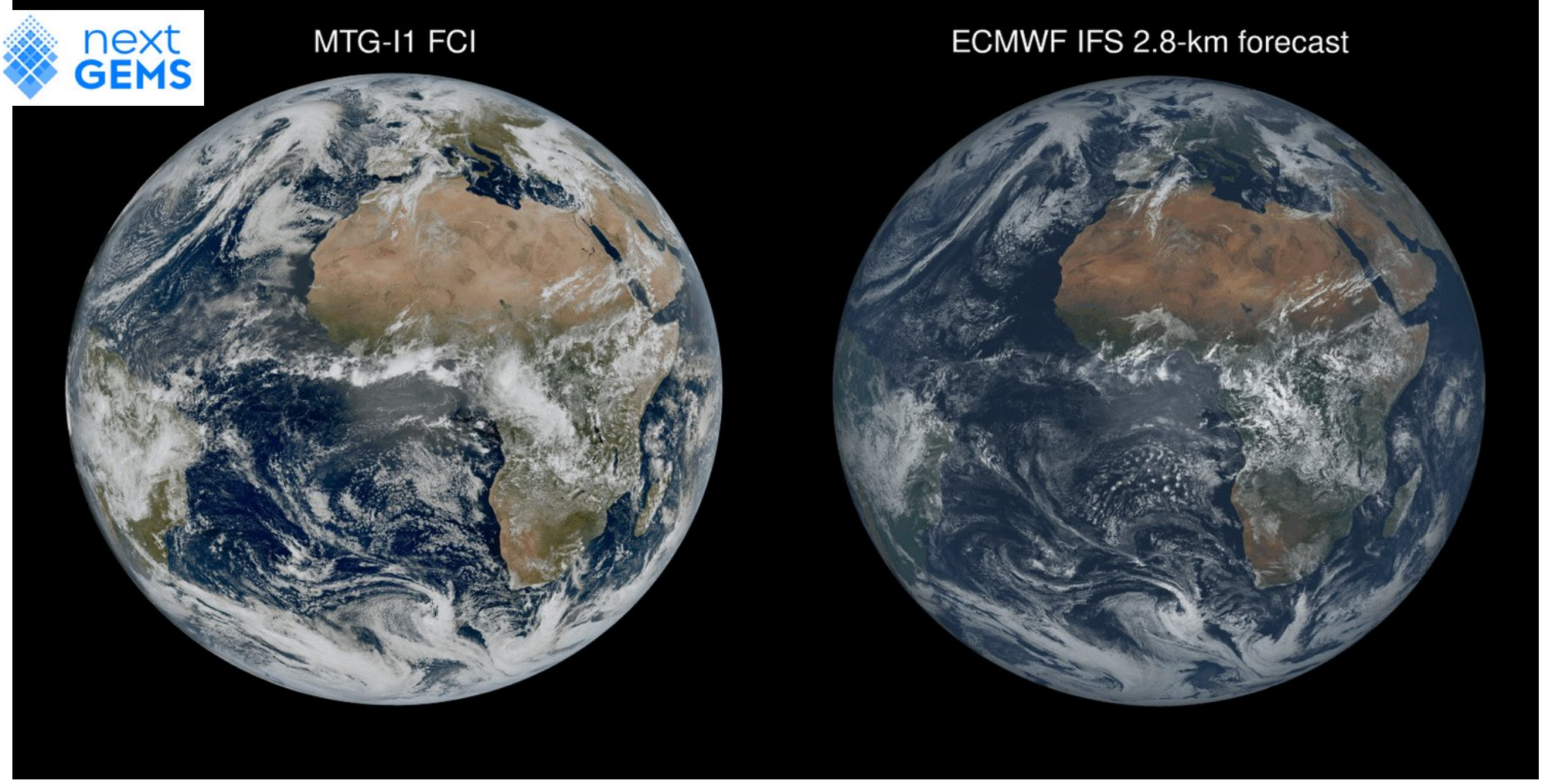

The first visible-light image from the MTG-FCI satellite from EUMETSAT (left) and a 12-hour simulation using ECMWF's Integrated Forecasting System (IFS) at 2.8km resolution (right), valid for March 18, 2023 at 12:00 UTC. Source: EUMETSAT/ECMWF

Acknowledgments:

POST field project was supported by the National Science Foundation with the grant ATM-0735121 and by the Polish Ministry of Science and Higher Education with the grant 186/W-POST/2008/0.

ACORES field project was supported by German Research Foundation DFG (grants SI 1543/4-1, WE 1900/33-1, WE 2757/2-1, and HE 6770/2-1) and with the Polish National Science Centre (grant 2013/08/A/ST10/00291).

EUREC4A field project was supported by by German Research Foundation, Max Planck Society, EU H2020 programme, many other institutions including Polish National Science Centre (grant 2018/30/M/ST10/00674)

NEXTGEMS received funding under the European Union's Horizon 2020 research and innovation programme (grant agreement No 101003470).

Some other research presented here was supported by the Polish National Science Centre and the University of Warsaw.